Chapter 1

Introduction

1.1 Introduction to Optical Lithography

As critical dimensions(CD's, also called "feature size") in the rapid development of the semiconductor industry have been continuously reduced, the improvement of optical lithography has played a very important role in the semiconductor industry. Lithographic requirements differ from chip to chip. The fabrication of DRAM chips has traditionally required the most advanced lithographic techniques, and the half-pitch (mainly the distance between near memory 'cells' on the chip) remains an important practical constraint in the fabrication of DRAMs. But more recently, the significant commercial pressure for increased performance and expansion of market size has resulted in the development of microprocessors, high-end logic large-scale integrated (LSI) circuits, and 'system-on-a-chip' LSI circuits that each use smaller-scale patterning than the contemporary generation of DRAMs.

The smallest CD that can be resolved is determined by optical diffraction and is mathematically represented in the Rayleigh criterion, which is expressed as a function of the exposing wavelength λ and the numerical aperture ($NA = n \sin\theta$), where n is the refractive index of the imaging medium and θ is the maximum acceptance angle. The resulting expression for the critical dimension is:

$$CD = K1\frac{\lambda}{NA} \quad (1.1)$$

where K1 is a scaling factor that accounts for variations in the lithography process. Such variations are present due to photoresist processing, coherence of the illumination and wavefront manipulation. Physical limitations constrain K1 to be greater than 0.5 and 0.25 for coherent and incoherent illumination, respectively [1]. When the projection system was first introduced, the required minimum CD was relatively large compared to the wavelength of the exposure light. The NA of the lens system used was also rather small. However, as the rate of device miniaturization has proceeded faster than the rate of reduction of the exposure wavelength, projection systems with higher resolving capabilities are now required. So, the lithographers must develop a number of novel techniques to extend optical lithography as the principal method of imaging.

The DOF is one figure of merit (FOM) that must be considered when attempting to optimize the resolution of an imaging system. The DOF is characterized as the usable range of field positions along the optical axis that result in minimal image degradation. The formula of the DOF is:

$$DOF = K2\frac{\lambda}{NA^2} \quad (1.2)$$

It is readily evident from equation (1.2) that an undesirable reduction in the DOF will occur when optimizing resolution through the use of short wavelengths or high NA. The formula of the DOF also includes a process dependent factor analogous to the factor incorporated into the Rayleigh criterion for resolution. The term K2 is introduced to account for all process variables not related to wavelength or NA, and is

typically K2 ≈ 0.5. A large DOF is desired in order to minimize the impact of defocus aberration on an imaging system [1].

1.2 Motivation

The use of RET has become an absolute necessity for the manufacture of advanced integrated circuits [2]. Unfortunately, each RET comes with its own set of layout limitations. For example,“forbidden pitches” for OAI and scattering bar processes, phase conflicts for alternating PSMs, or sidelobe printing for attenuated PSMs [3].Among numerous RETs, PSMs and OAI are the most widely investigated and practically applicable ones because of their cost-effectiveness to other enhancement approaches and compatibility with present manufacturing infrastructures. While high NA (>0.75) processes using partially coherent illumination can achieve sufficient resolution; they do not have sufficient overlapping DOF and also have large MEEF that do not allow partially coherent illumination to cover the entire pitch range. OAI easily provides the resolution and MEEF performance needed to image contact-hole for select dense pitch ranges, but suffers from very poor DOF in isolated regions. There is still a lot of understanding missing on the details of the implementation issues. Tedious simulation work must be done to avoid these drawbacks.

1.3 Resolution Enhancement Techniques

RETs modify the shape of the wavefront of an imaging system at the

illumination pupil and/or the imaging pupil by spatial filtering [4]. Some RETs are very similar to those used in microscope technology. To improve the resolution of an optical lithography system without introducing other impractical constraints (on, for example, wafer smoothness), several resolution-enhancement strategies have been proposed [5, 6, 7].

[Figure 1-1] shows a schematic view of a typical projection optical-exposure system. Such a system consists of several sub- systems, and resolution-enhancement ideas can be applied at various points.

(1) **Off-Axis Illumination :** OAI is a common RET method at the illumination plane. The illumination coherence in the spatial domain is an adjustable parameter that has influence on the imaging performance. The illumination is said to be partially coherent if a certain amount of spatial coherence exists. The amount of partial coherence is governed by the ratio of the NA of the condenser lens (NAi) to the projection lens (NAo). The so-called partial coherence factor, σ, is shown in **[Figure 1-2]**. An aperture is introduced in front of the light source to control the coherence factor. This aperture changes the effective size of the source. A circular aperture, as in the case of partially coherent illumination, refers to simple low pass filtering with a cut-off frequency determined by the numerical aperture of the condenser lens (NAc) and that of the projection lens. Only plane waves up to a certain amount of obliqueness can pass through the mask. By applying only oblique illumination, it is possible to change the minimum period of pattern whose first diffracted beam can pass through the projection lens. The zero order beam will pass through the edge of the projection lens, thus the minimum resolvable

period R' [8]is given by Equation (1.3)

$$R' = \frac{\lambda}{NA(1+\sigma_{obl})} \tag{1.3}$$

where σ_{obl} is angle of obliqueness in terms of σ .Equation (1.3) only gives the minimum resolvable period and not the real resolution. When only an oblique beam is utilized withσ_{obl} and proper resist, resolution can be achieved as per equation (1.3).

(2)**Phase Shift Mask :** Due to their binary nature, conventional binary masks either transmit or attenuate light without varying phase. Adding a phase-shifting function to binary masks may yield a higher resolution at the same or larger DOF. Thus, phase-shifting is a technique used to reduce the K1 parameter [9]. The enhancement is defined from the fact that both the amplitude and phase are used to store information about the image on the mask. The phase-shifting principle was first introduced in 1982 by Marc Levenson, but has since remained as a development technology. Recent enormous efforts have been made in industrial applications and production application has begun for special applications [10]. There are several different types of phase shift masks. The various types of masks are presented in **[Figure 1-3]**. Among them, alternating phase shift masks in **(b)**, the phase edge masks, and attenuated phase shift masks in **(d)** [11] - [13] are the most interesting in practical application.

(3)**Focus-Latitude Enhancement Exposure** : In 1987 lithography engineers at Hitachi invented a method for increasing the depth of focus, which they termed focus latitude enhancement exposure (FLEX). In FLEX several focal planes are

created at different positions along the light axis, and exposures are made using each focal plane. The method is shown schematically in **[Figure 1-4]**. For simplicity, only a single difference in the level of the substrate is assumed. As shown in this figure, two exposures are superposed in FLEX. One has a focal plane in the upper level and the other in the lower level. Each exposure is made in the same place on the substrate for the same mask pattern. For simplicity, only two focal planes are illustrated in this figure. However, there are no restrictions on the number of focal planes which can be used. **[Figure 1-5]** shows variations in the light-intensity distribution along the light axis. Image I is for the focal plane which lies on the lower level of the substrate while image II is for the focal plane on the upper level. Image I and II shows the superposed image obtained by adding the upper and lower level exposure planes.It can be seen that a sharp light intensity distribution is maintained over a wider focal range by superposing these two images.

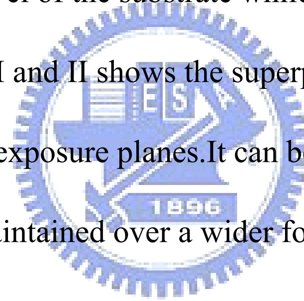

(4)**Lens Pupil-Filtering:** It is similar to the the FLEX method which uses mutiple exposures at different focus levels to obtain a deeper focal range, the lens pupil-filtering method is based on the intensity superposition in the axial direction, just like the phase-shifting method uses the phase-controlled amplitude superposition in the lateral direction.

Variations both in light amplitude distribution and in light intensity distribution are shown in **[Figure 1-5]** at three positions, $z = +\beta, 0, -\beta$, along the light axis. The result of the conventional exposure (the amplitude U_0) is shown in **[Figure 1-5](a).** The desired image profile can be obtained only at $z = 0$. Then, the amplitude superposition, as illustrated in **[Figure 1-5](b)**, is considered. First, the

amplitude U_I is obtained by moving the original focal plane for U_0 to axial position $+\beta$ with some phase change. Then, U_{II} is similar obtained by moving the focal plane and changing the phase to the opposite direction. Finally, the amplitudes U_I and U_{II} are superimposed. The superimposed amplitude and light intensity distributions are also shown in **[Figure 1-5](b)**.

The following results can be seen from**[Figure 1-5]**. First, the DOF is increased by axial image superposition just as in the FLEX method. To attain the same result[14] we can use the lens pupil which has the pupil function P'(r,z) as equation (1.4)

$$P'(r,z) = \cos(2\pi\beta r^2 - \frac{\theta}{2}) \cdot P(r,z) \tag{1.4}$$

$$P(r,z) = circ(r) \cdot \exp(2\pi i z r^2) \tag{1.5}$$

Here, r is the radial coordinate on the pupil plane normalized by the pupil radius, z is the focusing error normalized by $2\lambda/NA^2$, P(r,z) is the original pupil function, $\theta = 2\Delta\varphi - 8\pi\beta/NA^2$, $\Delta\varphi$ is phase change of the image of U_I and U_{II} of **[Figure 1-5]**, and circ(r) is the transmission distribution of the lens pupil(simple clear circle aperture).

The pupil function is physically considered as the amplitude transmission distribution at the lens pupil. Therefore, the modified pupil function P' (r,z) is obtained by just applying amplitude filtering at the original lens pupil.The principle of the pupil filtering method will discussed in Ch.3 of this thesis. This method is also called the "Super-FLEX".

1.4 Organization of This Thesis

The thesis includes four chapters. In chapter 1 , we make an introduction to describe the background of the optical lithography and the role in the semiconductor

industry that optical lithography is playing. In addition , we make a brief to describe simple concept of the optical lithography. Then , we describe the motivation of this thesis. Finally , we introduce four kinds of the well-known RETs. They are OAI, PSM, FLEX and lens pupil-filtering respectively.

In chapter 2 , we will first specify our simulation model and condition. Then , we will illustrate and define the parameters of image quality with mathematical formula or example.

In chapter 3 , we first explain the mechanism of Super-FLEX effect. Then, we use these two method of Super-FLEX to exposure the contact-hole pattern by simulation. And, we use a kind of the isolated contact-hole pattern design which has the function similar to Super-FLEX when using with OAI, and we also use the design to exposure contact-hole pattern by simulation . Finally, we will compare this design with Super-FLEX effect.

Finally, in chapter 4 , we will make a conclusion in the whole thesis.

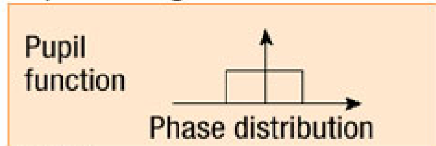

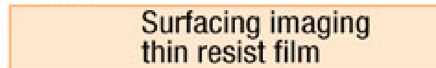

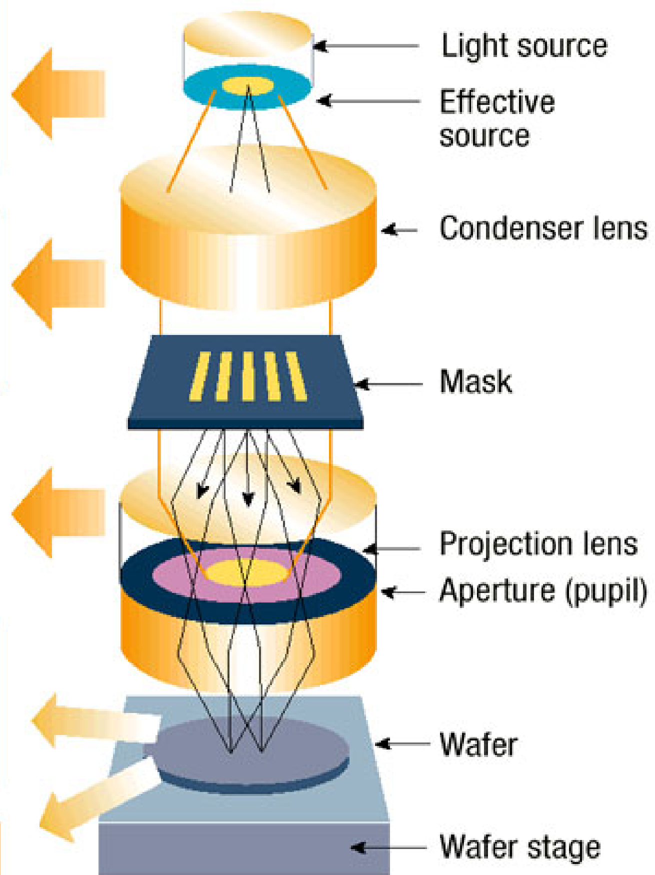

Figure.1-1 A schematic view of a typical projection optical-exposure system and resolution enhancement technologies.

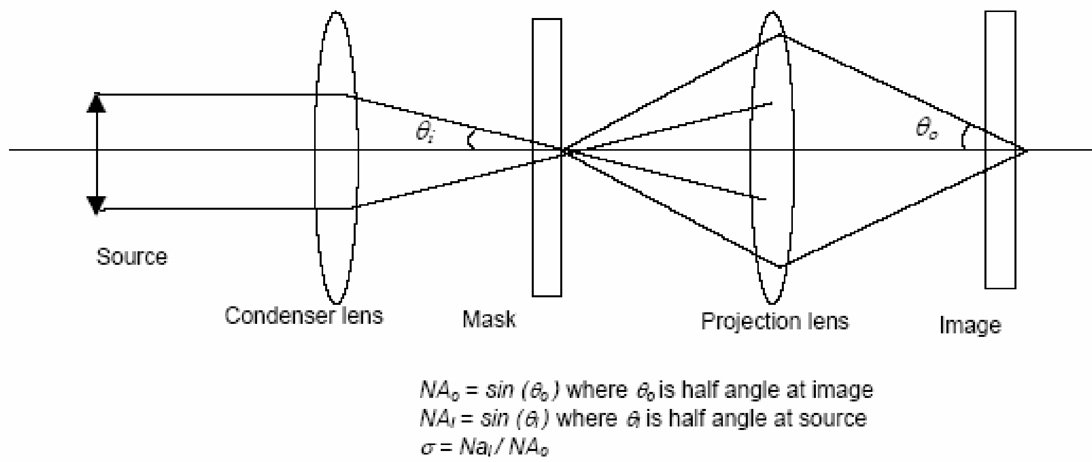

Figure.1-2 The definition of partial coherence factor, σ, and NA of the exposure system.

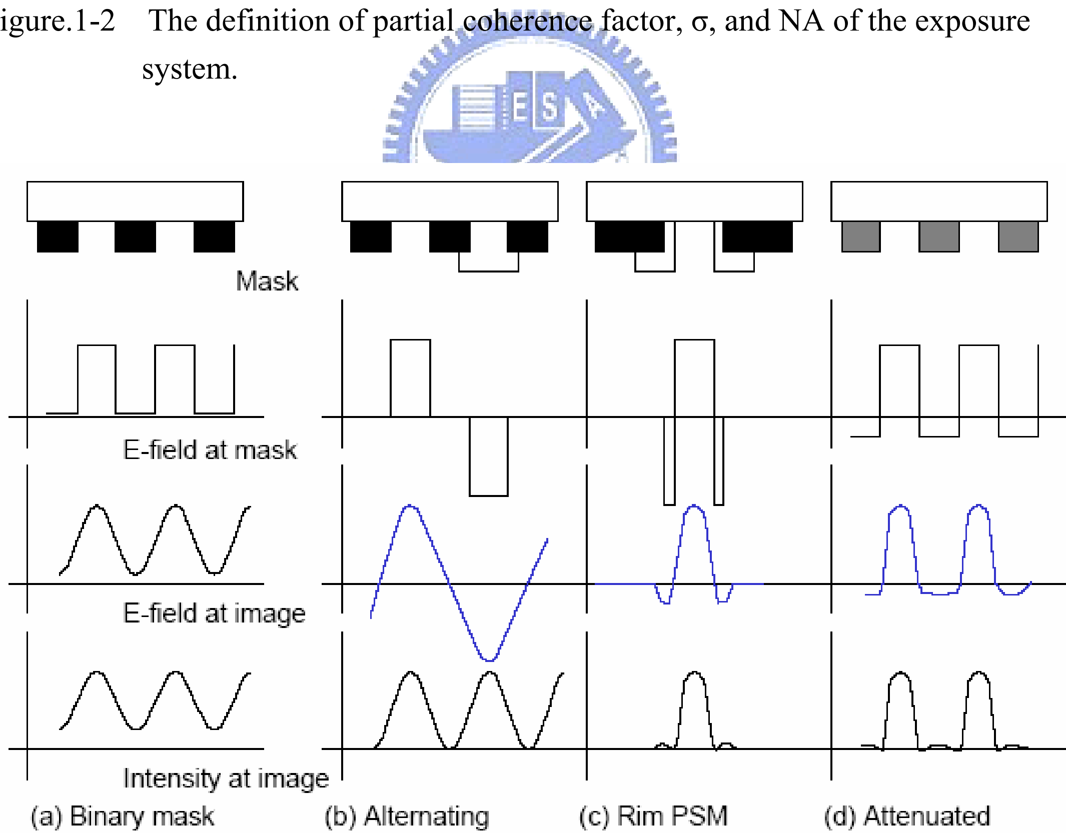

Figure 1-3 The various types of PSMs.

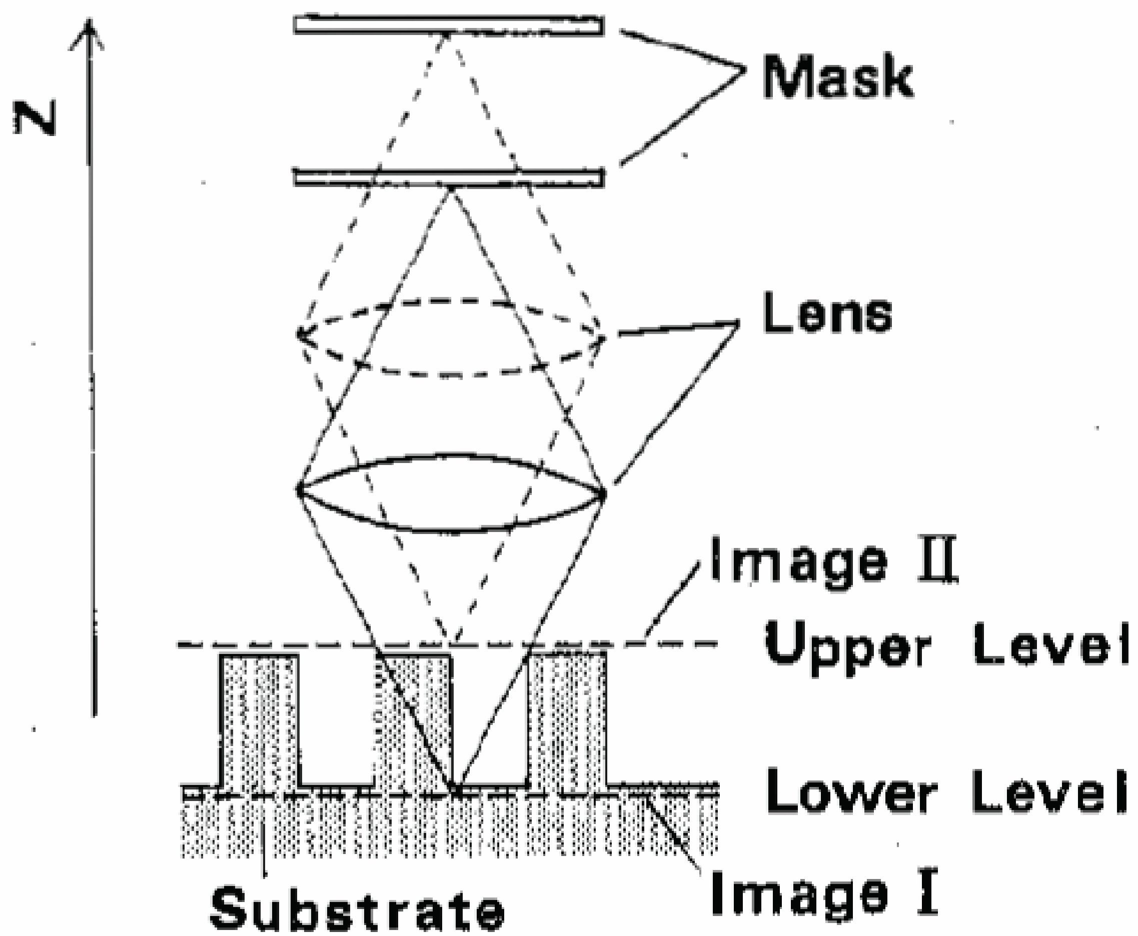

Figure 1-4 Shematic view of the FLEX method

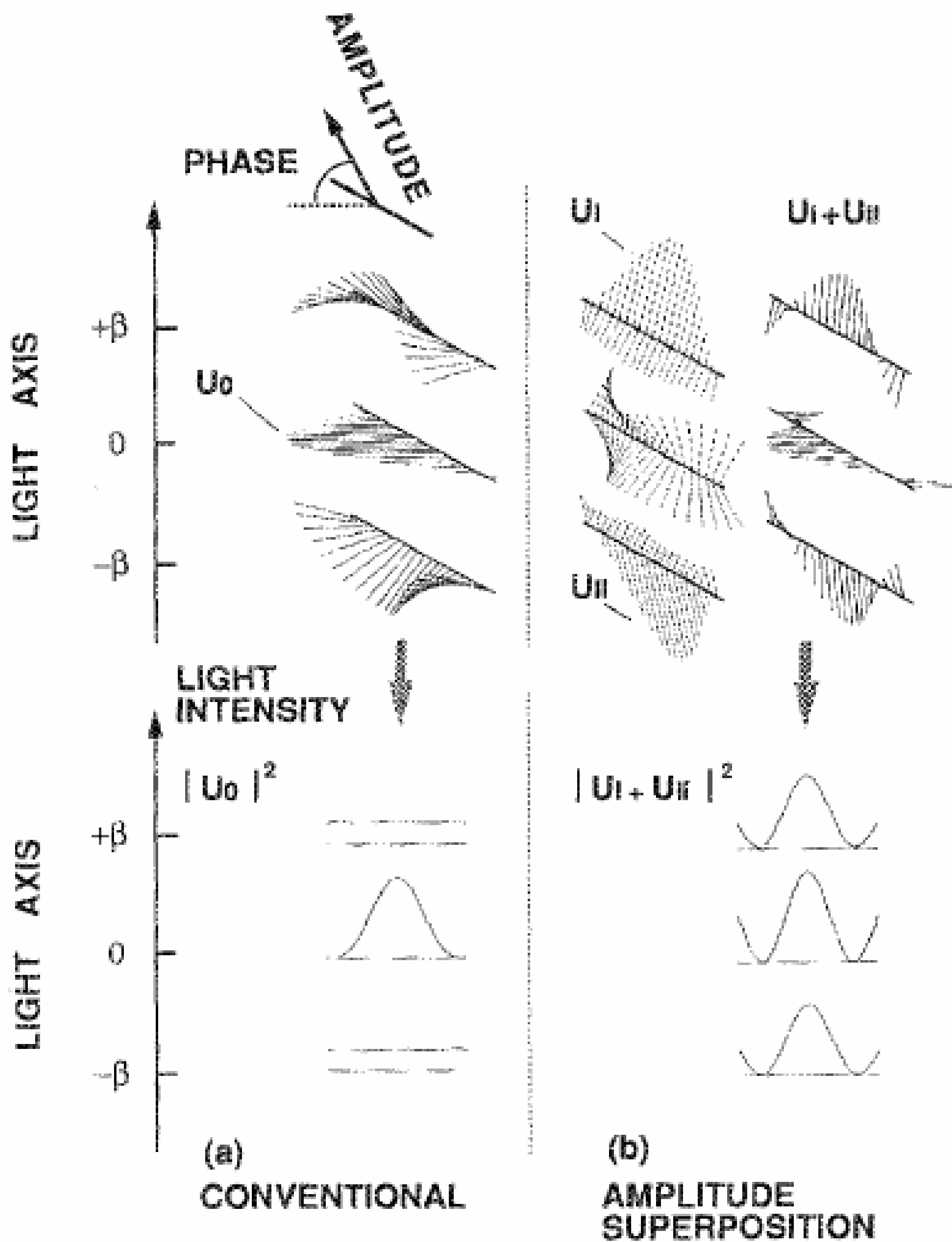

Figure 1-5 Variations in light amplitude and intensity distributions along the light axis. (a) Conventional, (b) amplitude superposition in axial direction.

Chapter 2

Models of Optical Lithography Imaging

2.1 The Optical Lithography Exposure System

As shown in the **[Figure 2-1]**, it is a picture of the major function of a stepper, and is closer to the real condition. And, the **[Figure 2-2]** is the crossection view of the optical lithography imaging. That will be more helpful for us to construct the imaging concept of optical lithography. When we have a good diagram, we will be enable to handle the point quickly.

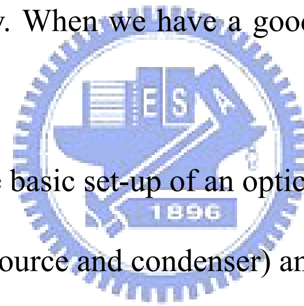

[Figure 2-3] sketches the basic set-up of an optical imaging system. It consists of the illumination optics (light source and condenser) an object (mask) and the projection optics (projector). The condenser ensures homogeneous illumination of the mask in the object plane of the projection system.

2.2 Models of Optical Imaging

Practically all lithographic systems employ Köhler illumination (the light source is imaged into the entrance pupil of the projection system). The projector maps the complex light distribution behind the mask to the image plane of the projection system where the wafer is placed. Both condenser and projector are combinations of lens elements, which are optimized to perform their role in the imaging system.

In this thesis, we omit the magnification of the lens, all formulas are

considering the 1:1 projection systems. We start with a description of the basic model for a diffraction-limited, 1:1 projection system with coherent illumination parallel to the optical axis.

The method used in Fourier optics is to Fourier-transform the complex amplitude distribution of the object $U_{obj}(x,y)$, to calculate the propagation of the Fourier-components in the optical system and to obtain the complex amplitude distribution in the image plane $U_I(x,y)$ by an inverse Fourier transform [15]. This procedure is summarized in the basic equation for the calculation of optical images.

$$U_I(x,y) = F^{-1}[H(f_x, f_y)F[U_{obj}(x,y)]] \quad (2\text{-}1)$$

Here F and F^{-1} denote a Fourier transform and inverse Fourier transform respectively. The complex amplitude distribution of the object $U_{obj}(x,y)$ is determined by the mask transparency distribution . The coherent transfer function of the optical system $H(f_x, f_y)$ describes the propagation of the individual Fourier components inside the system. It can be calculated from the pupil function of the projection system.,where fx, fy is refer to the spatial frequencies dmoain coordinates of the object .

Formally, the Fourier transformation of the object corresponds to a plane wave decomposition, where the spatial frequencies are, apart from a factor 2π, the transverse components of the plane wave propagation vector ($kx=2\pi fx$, $ky=2\pi fy$). Sometimes , for convenience we use the direction cosine σ_x, σ_y and σ_z of the plane waves or Fourier components respectively. They are related to the spatial frequencies by:

$$\sigma_x = \lambda \cdot f_x, \quad \sigma_y = \lambda \cdot f_y, \quad \sigma_z = (1-\sigma_x^2-\sigma_y^2)^{1/2} \qquad (2\text{-}2)$$

Finally, the intensity distribution in the image plane *I(x,y)* is calculated by:

$$I(x,y) = U_I(x,y)\,[U_I(x,y)]^* \qquad (2\text{-}3)$$

When an opaque mask is illuminated by a plane wave which propagates parallel to the optical axis, $U_{obj}(x,y)$ will be identical with the complex mask transparency *t(x,y)*. That is:

$$U_{obj}(x,y) = t(x,y) \qquad (2\text{-}4)$$

The object spectrum is obtained by an analytical Fourier transform of *t(x,y)*. Therefore, our simulation program is calculed the amplitude distribution of the image by subdivided the mask into rectangular areas of constant transparency.

The aperture stop of a projection system has a finite size and thus accepts only Fourier components of the object spectrum inside a certain range. The maximum acceptable angle α specifies the *NA* of the system according to NA = $(\sigma_x^2 + \sigma_y^2)^{1/2}$ = sin α. .Whether a specific Fourier component is transmitted or blocked by the projection system depends on the shape of the projector entrance pupil . This effect is taken into account through the coherent transfer function $H(\sigma_x,\sigma_y)$.

2.3 The Process Window and Energy Latitude

In the process from exposure to development，for the reason to get the required CD we must confirm our dose and focus at constant.But it is usually affected by the accurancy and stability of the stepper, the light dose and the focus may deviate from our setting value, and it will lead to the distortion of the image quality. If it is in the range of our tolerance, then the inaccurancy of the stepper is considered to be

acceptable. We first must choose our CD target to determine the DOF of the process. If the shift of CD which in the range of n% is acceptable, then the spec of maximum CD is (1+n%)CD and the spec of minimum CD is (1-n%)CD . Then we can change the exposure dose or defocus , and we can get a matrix chart like **[Figure 2-4]**, we call this "E-D window"(Energy-Defocus window)(or Bossong Plot, like a smile as the **[Figure 2-5]**), simultaneously we can pick the region where the CD is in the spec. By properly fitting we can get the **[Figure 2-6],** and then we can get the max defocus range at the constant Energy Latitude (EL), and the range is the DOF of the process. The rectangle inner region that is surrounded by the EL and DOF is also called the "process window".

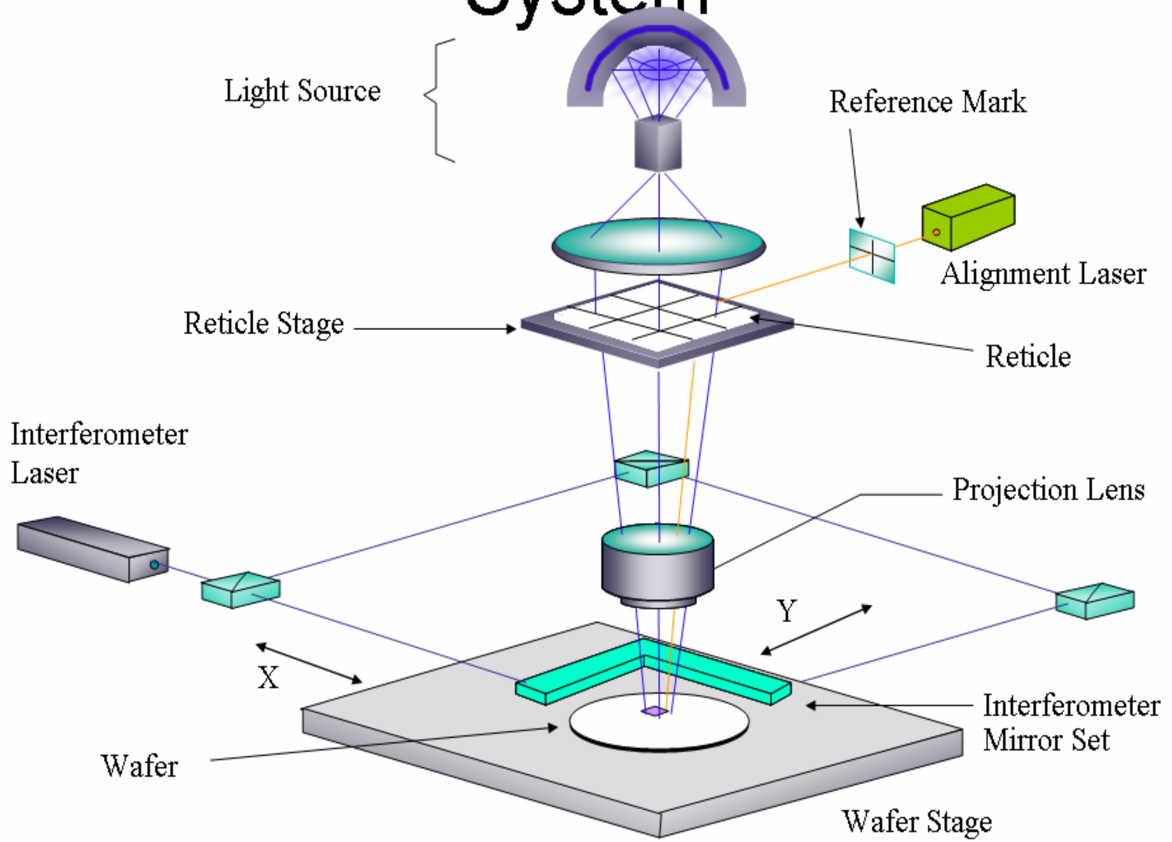

Figure 2-1 The optical lithography exposure and alignment system in a stepper

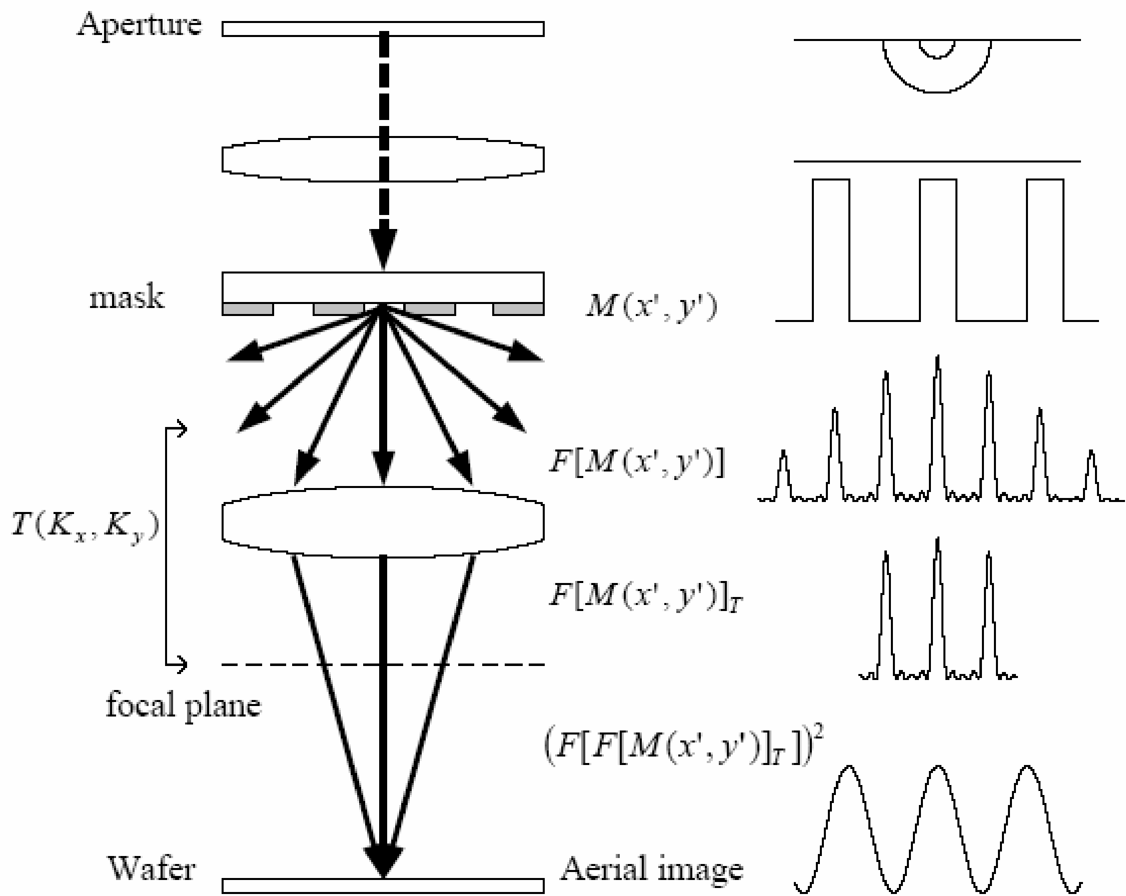

Figure 2-2 Crossection view of the optical lithography exposure system

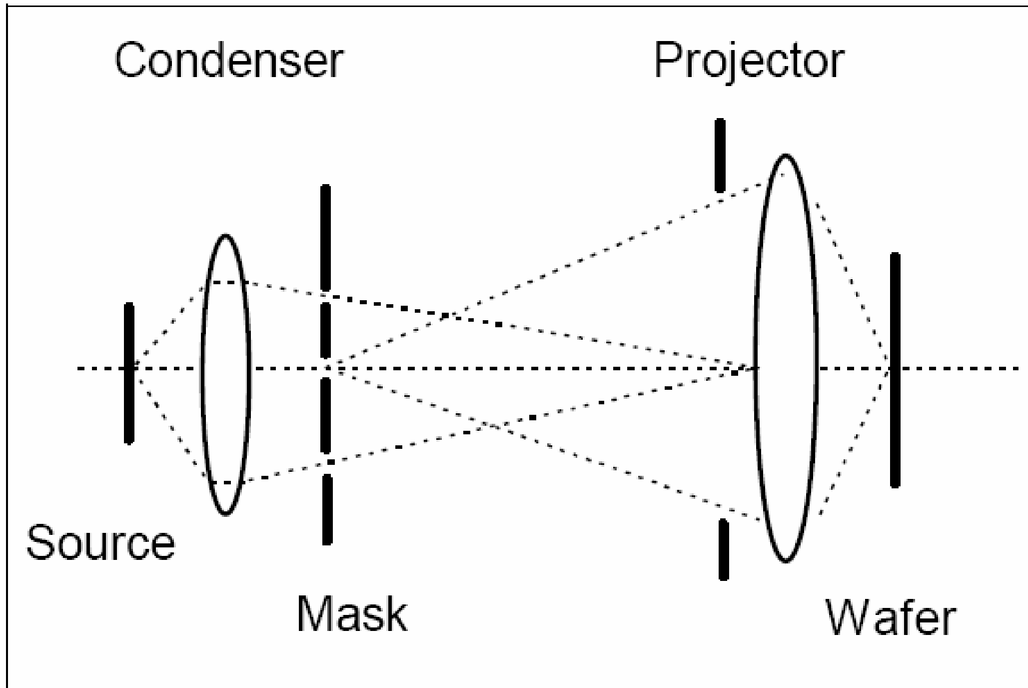

Figure 2-3 Basic setup of the optical imaging system

ES

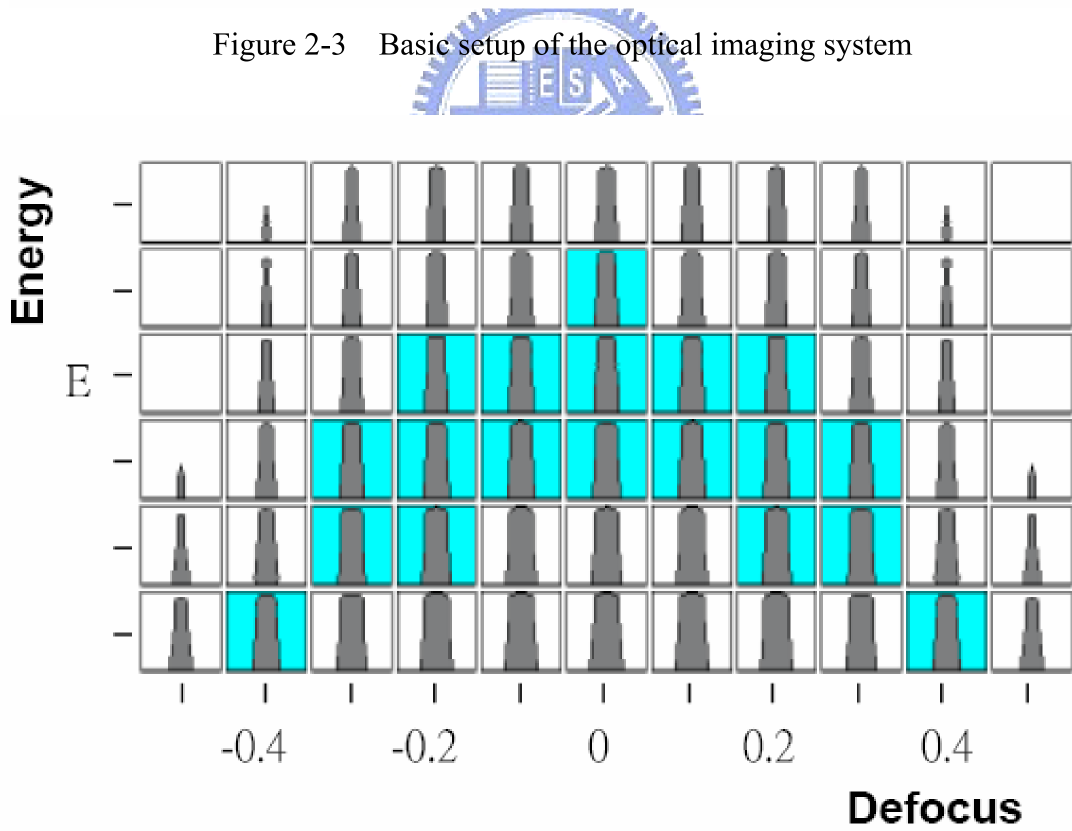

Figure 2-4 The E-D window chart

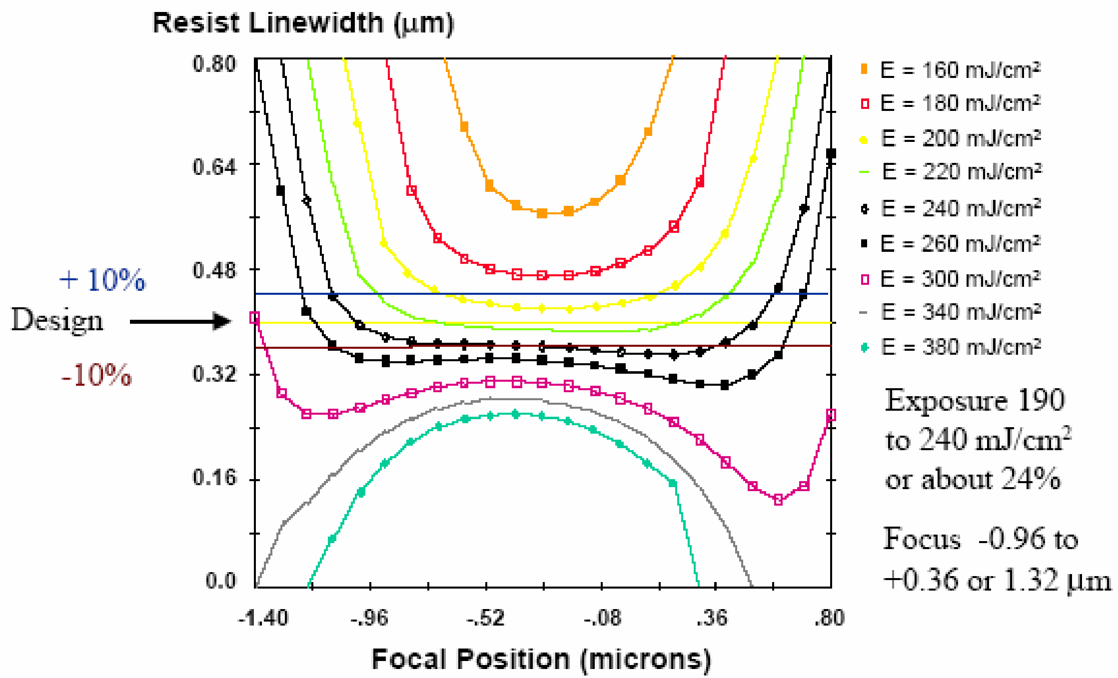

Figure 2-5 The Bossong Plot

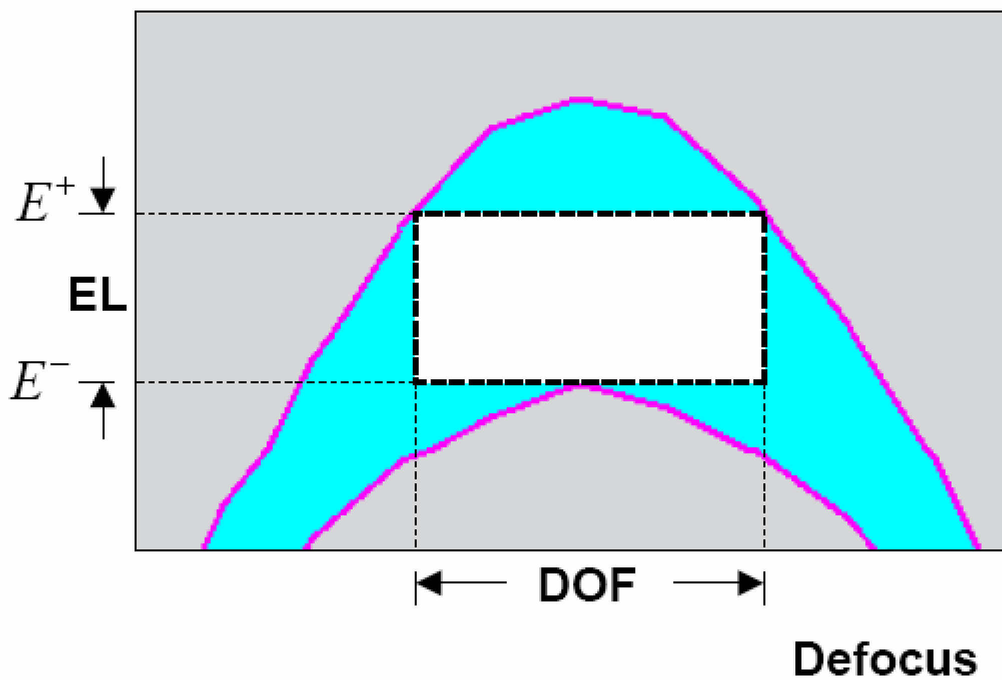

Figure 2-6 The chart to determine process window

Chapter 3

The Simulation of Super-FLEX

3.1 The Super-FLEX

The meaning of the “Super-FLEX” effect is that we can improve the depth of focus and resolution by the amplitude superposition for multiple image along the light axis and the phase-control between them. The mechanism of Super-FLEX can be described by Fourier optics. It can be mathematically expressed as follows under coherent illumination. As in the **[Figure 3-1]**, we can calculate the image amplitude distribution $U_0(x,y)$ by Fourier optics[15]. The result is the equation (3.1):

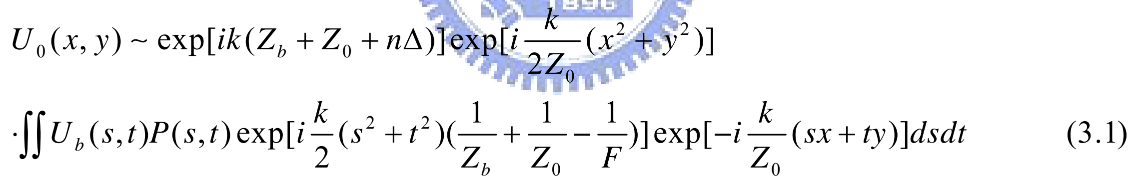

$$U_0(x,y) \sim \exp[ik(Z_b + Z_0 + n\Delta)]\exp[i\frac{k}{2Z_0}(x^2+y^2)]$$

$$\cdot\iint U_b(s,t)P(s,t)\exp[i\frac{k}{2}(s^2+t^2)(\frac{1}{Z_b}+\frac{1}{Z_0}-\frac{1}{F})]\exp[-i\frac{k}{Z_0}(sx+ty)]dsdt \qquad (3.1)$$

where λ is the wavelength of the light source, *k* is the wavenumber, Δ is the thickness of the lens, P(x,y) is the pupil function of the lens, *F* is the focal length of the lens.

If we exchange the $U_b(x,y)$ with the Fourier transform of the mask patterns (or we can say the spatial frequency domain image of the mask patterns), and normalize all z-direction term by $2\lambda/NA^2$, and put the term that before the integral into one term exp(i φ (z)), then we can get the similar form like equation (3.2):

$$U_0(x,y,z) = \exp[i\phi(z)]\iint a(f_x,f_y)P(|f|,z)\exp[2\pi i(f_x x + f_y y)]df_x df_y \qquad (3.2)$$

where $a(f_x,f_y)$ is the Fourier transform of the mask patterns, and $|f|$ is the amplitude of the spatial frequency.

When we apply the Super-FLEX effect to our exposure system, the equation will become:

$$U'(x,y,z) = \exp[i\phi(z)]\iint a(f_x,f_y)\cdot\cos(2\pi\beta|f|^2-\theta/2)P(|f|,z) \cdot\exp[2\pi i(f_x x+f_y y)]df_x df_y \qquad (3.3)$$

where both β and θ are the same as in the equation (1.4) of Ch.1.

There are two methods to carry out the Super-FLEX effect, one is lens pupil filtering method[16][17] and the other is mask modulation method[18]. Both methods make the amplitude superposition with arbitrary β(half the distance between two focal planess) and θ (the phase difference between two images) possible.

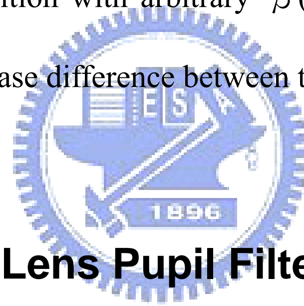

3.2 Super-FLEX by Lens Pupil Filter

The principle of the lens pupil filtering method is illustrated in **[Figure 3-2].** In the conventional optical system, its high spatial frequency components are simply cut by the pupil. The projected image exhibits strong defocusing dependence. In the lens pupil filtering method, the Fourier transform of the mask is modified after being transmitted through the amplitude filter. This enables the image superposition, and an image with a steep profile is obtained over a wide focal range. The effect of amplitude superposition depend on the distance between the two focal planes and the phase difference between them; these parameters can arbitrarily be set by changing β and θ in the filter

distribution. This can also be regarded as the change in the spatial frequency composition of the images after being transmitted through the filter. Various transmission distribution with different β and θ values are investigated to obtain the best imaging performance.

If we only think about one dimension, the filtering function of the lens pupil will be $\cos(2\pi\beta f^2 - \theta/2)$, and the valid value of the normalized spatial frequency f is in the range of [-1,1] (when using coherent illumination). **[Figure 3-3]** shows some typical curves of $\cos(2\pi\beta f^2 - \theta/2)$, when we set $\theta = 0$. We can see that when the value of β is increased, the curve will have more oscillations, and the central region will be thinner; and the curve will become more smooth when the value of β is decreased. So, we can predict that β will affect the efficient portion of the passing light. **[Figure 3-4]** shows some typical curves of $\cos(2\pi\beta f^2 - \theta/2)$, when we set $\beta = 1$. We can see that when the value of θ is changed, the curve will not have more oscillations, and just like the middle point is moving down or up. So we know that θ is the primary parameter to determine the shape of the curve.

[Figure 3-5] shows the E-D curve of 100nm contact-hole using binary mask (BIM) with conventional illumination. And **[Figure 3-6]** shows the E-D curve of 100nm contact-hole by lens pupil filtering method using BIM with the conventional illumination . Here, the parameter β is 0.67 and θ is 235 (degree), **[Figure 3-7]** is the 2-D contour and 1-D profile of this $\cos(2\pi\beta f^2 - \theta/2)$ curve.

3.3 Super-FLEX by Mask Modulation Method

The second method to carry out Super-FLEX effect is by mask modulation method. In the lens pupil filtering method, the Fourier transform image is modified after being transmitted through the filter. Instead of applying the filter, the mask modulation method use a mask that creat this modified Fourier transform image itself at the lens pupil, and we also can obtain the Super-FLEX effect without using the pupil filter. Such a mask pattern can be easily obtained by the inverse Fourier transform of the modified Fourier transform image, at least for coherent illumination. In other word, the the mask pattern is modified so that its Fourier transform becomes $a(f)\cdot\cos(2\pi\beta f^2 - \theta/2)$, where $a(f)$ is still the Fourier transform of the original mask pattern. The principle of the mask modulation method is illustrated in **[Figure 3-8]**. For the contact-hole, the pattern is just a simple square so its 2-D Fourier transform is easily calculated. As the Fourier transform image of the original mask pattern is obtained, and it is multiplied by $\cos(2\pi\beta f^2 - \theta/2)$. The final mask pattern is obtained as the inverse Fourier transform of this multiplied image. The modulations in both the amplitude and the phase are introduced because we will adjust the parameters β and θ to let the $\cos(2\pi\beta f^2 - \theta/2)$ curve go through the zero point in the range [-1,1].

Think about the 1-D condition, the modulated pattern $M'(x)$ is converted from the original pattern $M_0(x)$ by:

$$M'(x) = F^{-1}[\,F\{M_0(x)\}\cdot\cos(2\pi\beta|f|^2 - \theta/2)\,] \tag{3.4}$$

where F expresses the Fourier transform.

For example, think about the 1-D condition the contact-hole pattern will become the “rectangle function”, the “rectangle function” is a function that is 0 outside the interval [-L/2, L/2],where L is the feature size, and unity inside it, notated as rect(x/L). So, we will find the answer of $F^{-1}[\ F\{\ \mathrm{rect}(x/L)\}\cdot\ \cos(2\pi\beta|f|^2-\theta/2)\ ]$. Fortunately we can get the answer by table finding[19]. The whole formula is:

$$M'(x)=\frac{1}{2}\left\{\begin{array}{l}(u+v)\left[FresnelC\left(\frac{x+\frac{L}{2}}{\sqrt{\beta}}\right)-FresnelC\left(\frac{x-\frac{L}{2}}{\sqrt{\beta}}\right)\right]+\\(u-v)\left[FresnelS\left(\frac{x+\frac{L}{2}}{\sqrt{\beta}}\right)-FresnelS\left(\frac{x-\frac{L}{2}}{\sqrt{\beta}}\right)\right]\end{array}\right\} \qquad (3.5)$$

, where $u=\cos(\theta/2)$ and $v=\sin(\theta/2)$, *FresnelC* and *FresnelS* is the Fresnel cosine integral and Fresnel sine integral respectively. And the tedious formula can be calculated by computer program fast and very precisely. The 2-D case also can be solved by the same technique and is easy for computer program ,but just take a little more time to get the numeric data.

As the same parameters with the lens pupil filtering method, we set the parameters as $\beta=0.67$ and $\theta=235$ degree, and the result is shown in **[Figure 3-9]**. The **[Figure 3-10]** is our modified design according to the result of the modulated pattern, it is symmetric to x and y axis. **[Figure 3-11]** shows the E-D curve of the 100nm contact-hole pattern which is modified by the result of the modulated pattern.

3.4 Super-FLEX and OAI

When we use the modified modulated pattern with OAI, the performace such like the DOF is obvious not good ,it is shown in **[Figure 3-12]** .

We know that coherency is important to the resolution of optical lithography, obviously it is also important in the mask modulation method. For coherent illumination, the image in the pupil plane is just obtained by the Fourier transform of the mask pattern. For partial coherent illumination, the image in the pupil plane is obtained by superposing plural Fourier transform images with various center shifts according to the locations of point sources consisting the effective light source.Consequently, the imageing characteristics generally vary.

For this reason, we try to design a different method , and the purpose is to keep the advantage of Super-FLEX but using OAI. Because the DOF of dense contact-hole is better than conventional illumination except some problematic pitch that people usually say “forbidden pitch”[20].

[Figure 3-13] is our design,the main concept of the design is combination of the use of optimally placed phase-shifting assist feature(AF) and an optimum OAI condition[21]. It can generate a phase apodizing distribution over the pupil plane. This design is analogous to the apodizing phase and amplitude pupil filter instead of using a real pupil filtering lens. And the design is based on the principle of approximating the inverse Fourier transform of an apoding pupil function. Follow is the brief description about the principles under partially coherent illuminations.

For coherent illumination, the diffraction distribution on pupil plane is obtained by the Fourier transform of mask pattern[15]. For partially coherent illumination, the

diffraction distribution on pupil plane is obtained by superposing Fourier transform of mask pattern with various off-axis source illumination points. **[Figure 3-14]** shows a conceptual view of an optical projection system with partially coherent illumination used for this analysis. Each of the illumination source point can be associated with a coordinated pair (f_{sx} , f_{sy}) that is corresponding to a specific location of diffraction distribution on the lens pupil plane. When the condition is the on-axis coherent illumination, then the point source is assumed to be (f_{sx} , f_{sy}) = (0, 0). For a partially coherent source point where (f_{sx} , f_{sy})is not (0, 0), we can make the approximation that the optical projection system has a center shift such that the Fourier transform images of the mask due to the illumination source point, s , is described by a shifted function of the Fourier transform of the mask function under cohenert illumination, that is $a(f_x - f_{sx}, f_y - f_{sy})$. According to Abbe method of imaging, the intensity distribution on the image plane can therefore be described mathematically by follow :

$$I(x', y') = \left| \int \int_{-\infty}^{\infty} a(f_x - f_{sx}, f_y - f_{sy}) P(f_x, f_y) \exp[-2\pi i (f_x x + f_y y)] df_x df_y \right|^2 \qquad (3.6)$$

where I (x',y') is the intensity distribution on the image plane by one partial coherence point source.

[Figure 3-15] is the Fourier transform of our mask ,and is also the image of the mask on the pupil plane. When we use OAI , we can calculate the image of the mask on the pupil plane by equation (3.6) , and it will look like **[Figure 3-16].** It is interesting that the image on the pupil plane looks like that of rim-type PSM with conventional illumination. The principle of rim-type PSM design is mask modulation

method. So, we presume our design combine with OAI have the similar performance to rim-type PSM with conventional illumination.

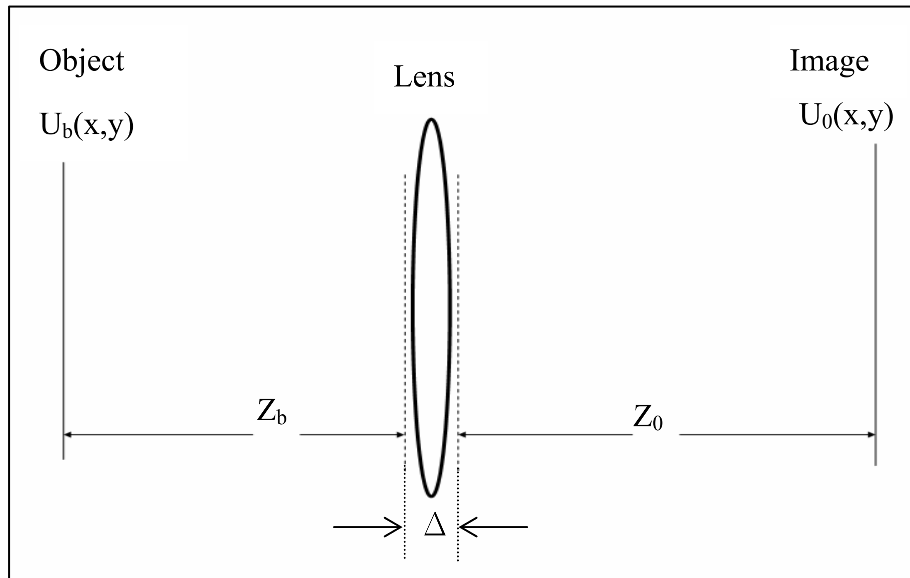

Figure 3-1 The simplified calculation model of Super-FLEX .

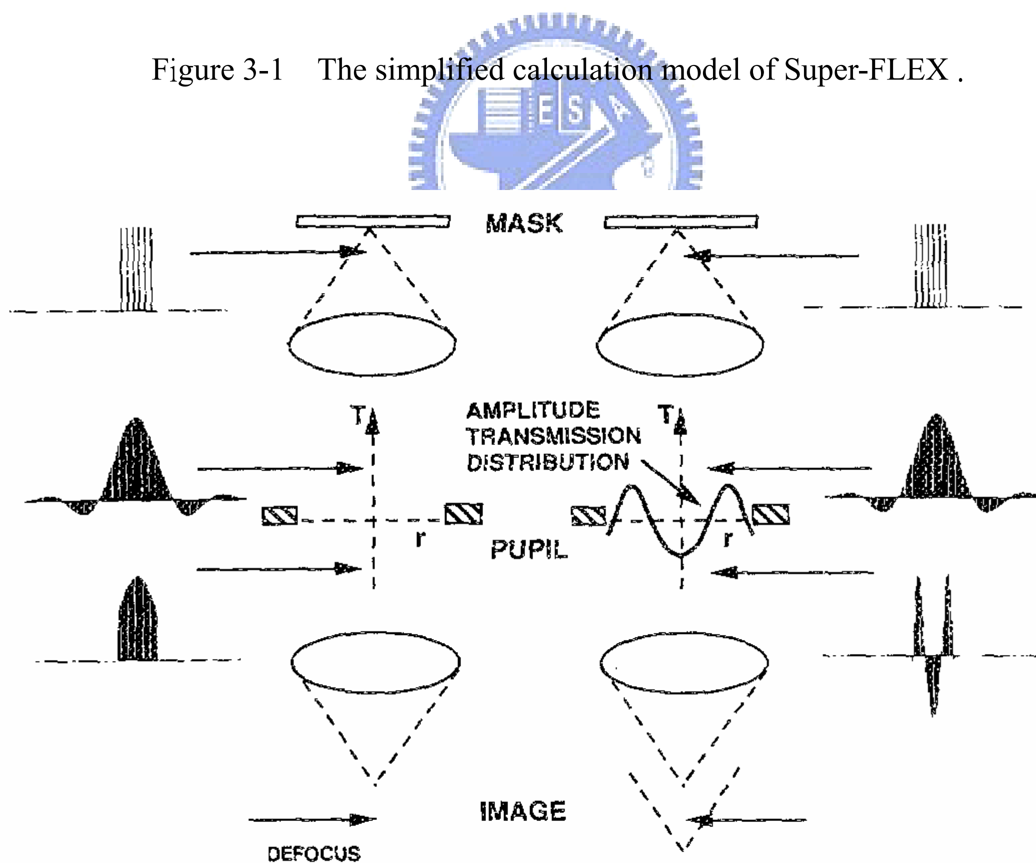

Figure 3-2 Principle of the pupil filtering method .

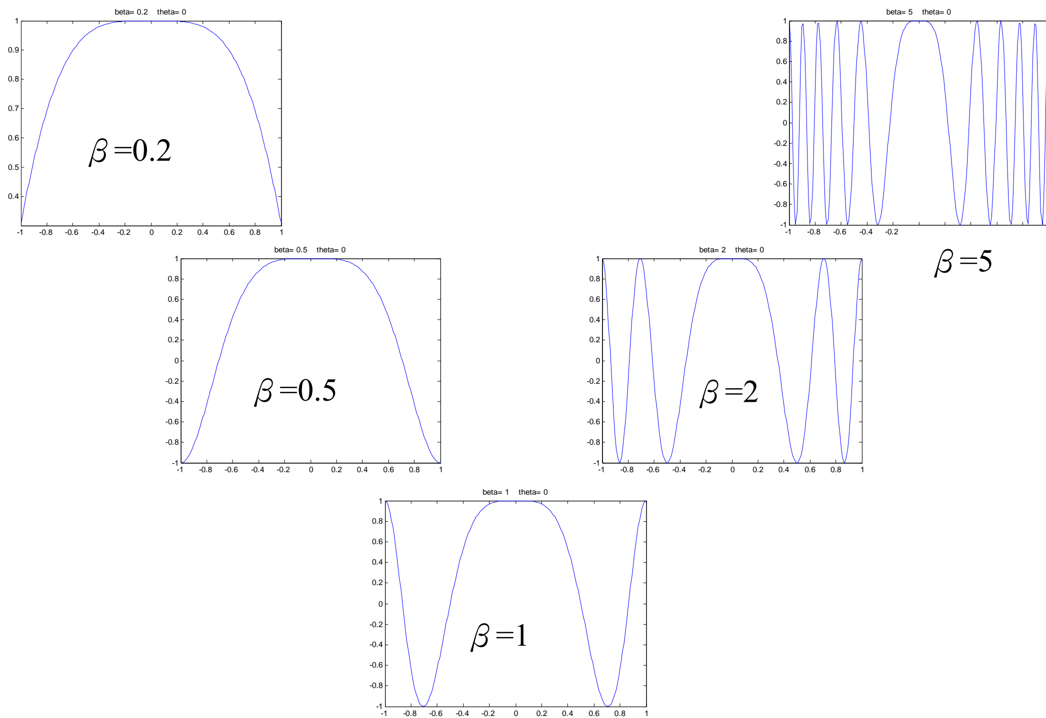

Figure 3-3 Some typical curves of $\cos(2\pi\ \beta f^2 - \ \theta/2)$ when $\theta=0$.

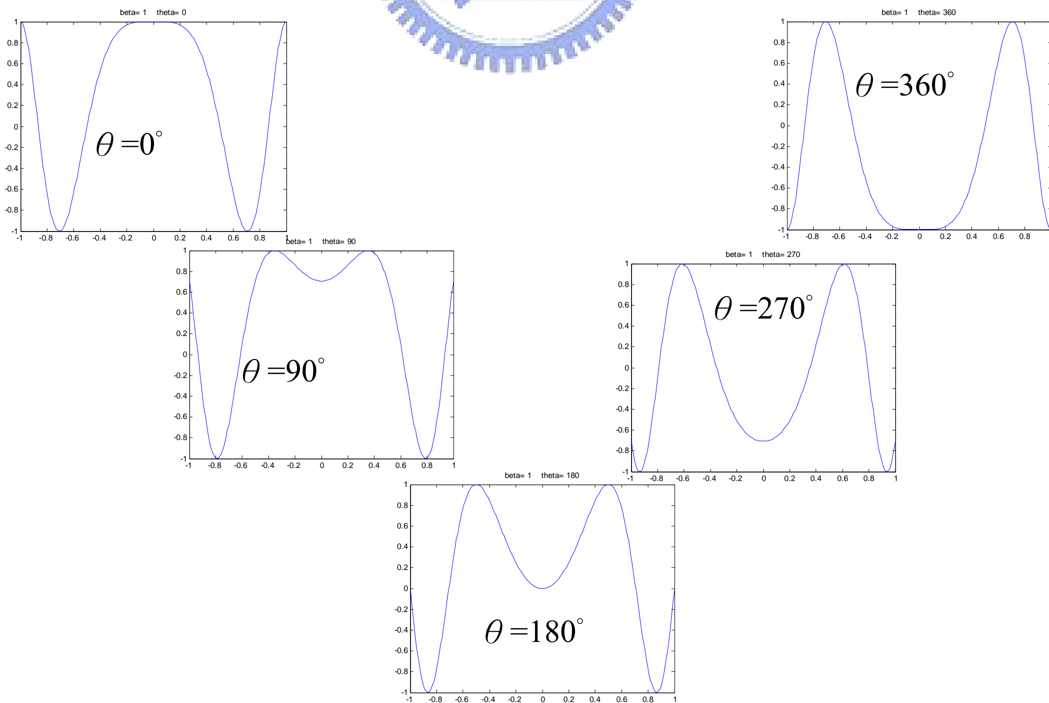

Figure 3-4 Some typical curves of $\cos(2\pi\ \beta f^2 - \ \theta/2)$ when $\beta=1$.

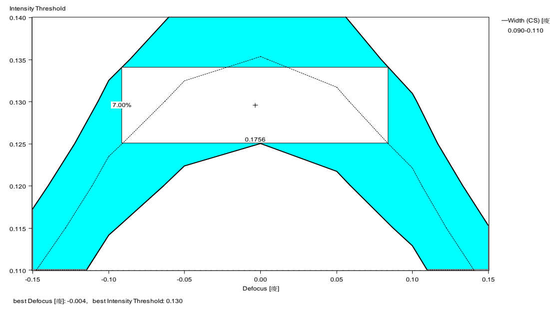

σ =0.1 ,

DOF= 0.1756 μm

best Intensity_threshold = 0.130

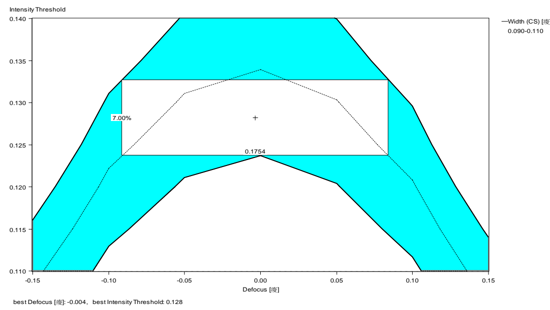

σ =0.2 ,

DOF= 0.1754 μm

best Intensity_threshold = 0.128

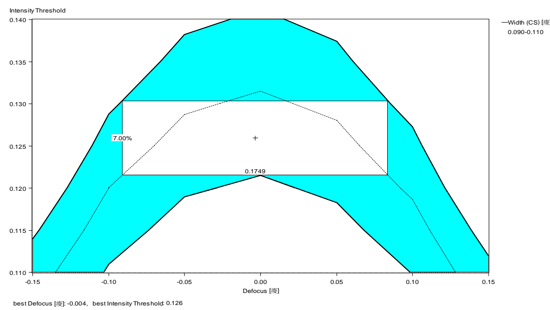

σ =0.3 ,

DOF= 0.175 μm

best Intensity_threshold = 0.126

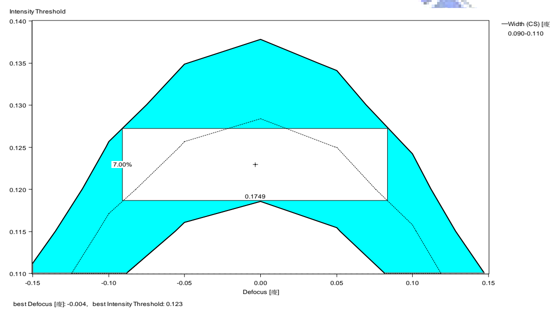

σ =0.4 ,

DOF= 0.1749 μm

best Intensity_threshold = 0.123

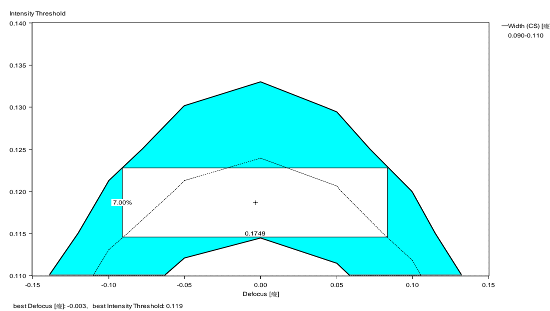

σ =0.5 ,

DOF= 0.1749 μm

best Intensity_threshold = 0.119

Figure 3-5 E-D curve of 100nm contact-hole using BIM with conventional illumination, set EL = 7% .

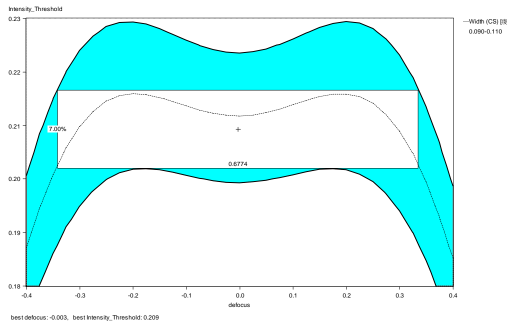

σ =0.1 ,
DOF= 0.6774 μm
best Intensity_threshold = 0.209

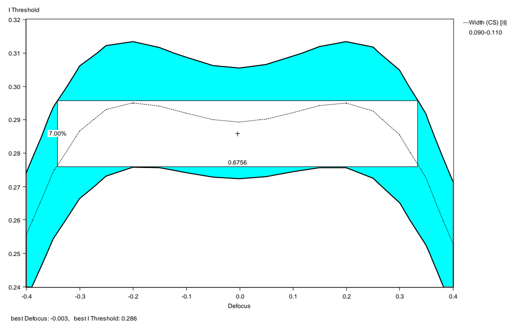

σ =0.2 ,
DOF= 0.6756 μm
best Intensity_threshold = 0.286

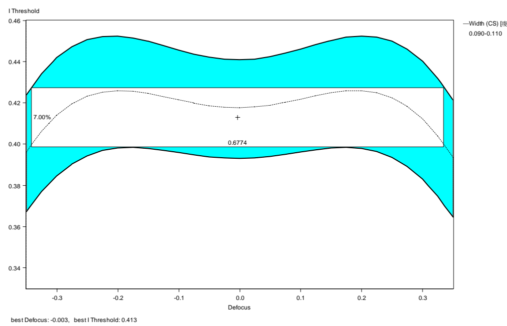

σ =0.3 ,
DOF= 0.6774 μm
best Intensity_threshold = 0.413

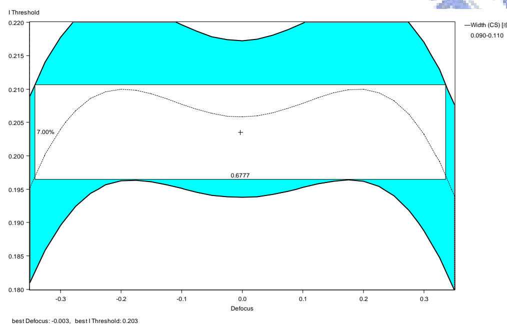

σ =0.4 ,
DOF= 0.6777 μm
best Intensity_threshold = 0.203

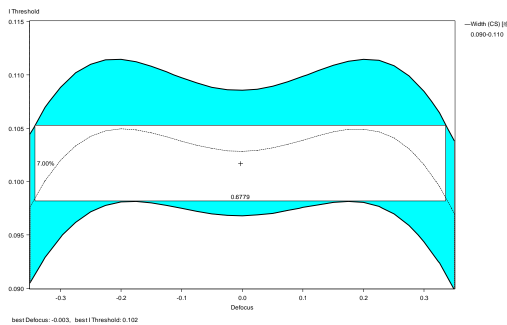

σ =0.5 ,
DOF= 0.6779 μm
best Intensity_threshold = 0.102

Figure 3-6 E-D curve of 100nm contact-hole by lens pupil filtering method using BIM with conventional illumination .
(NA=0.75, EL = 7%, β = 0.67, θ = 235)

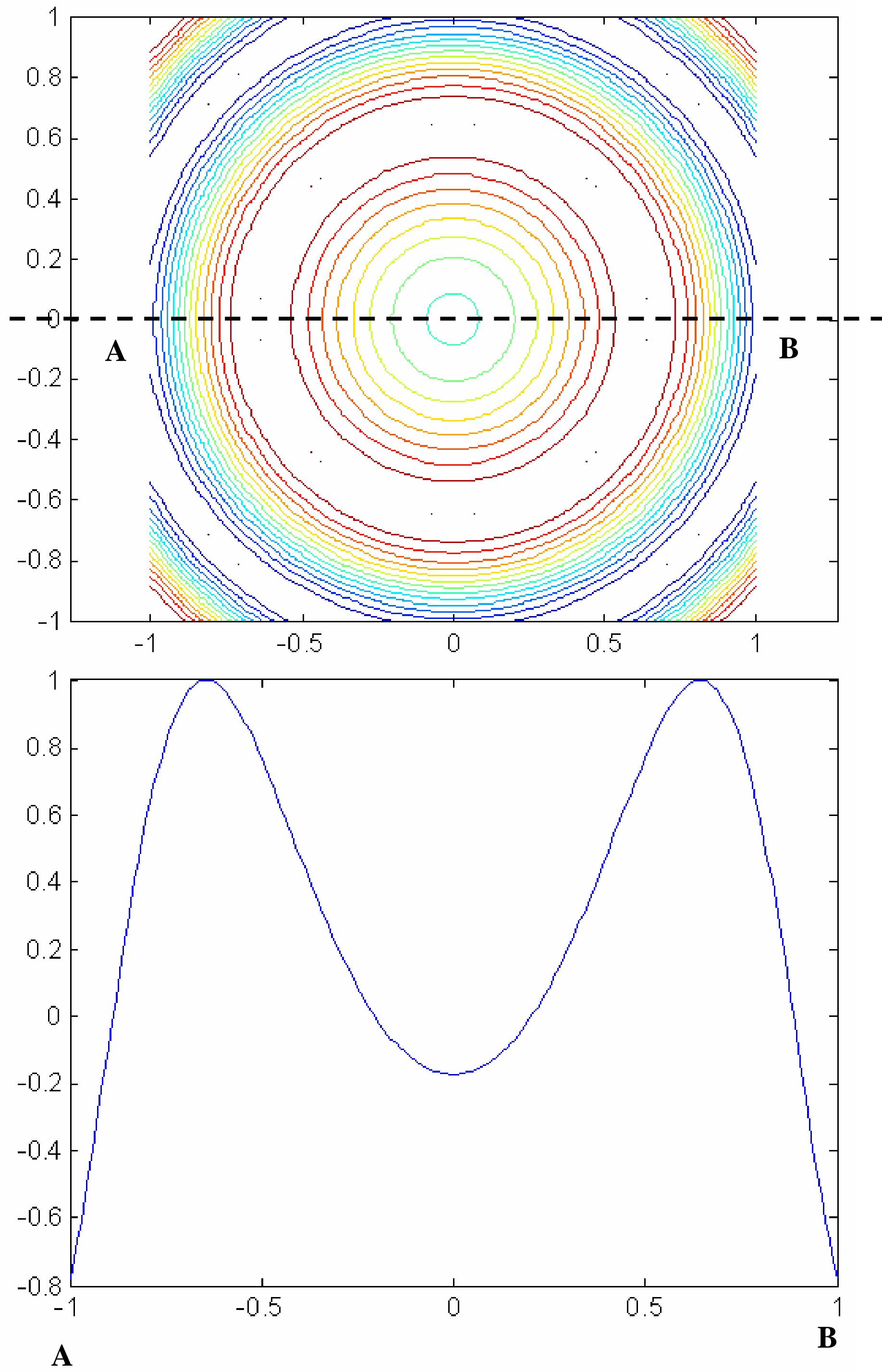

Figure 3-7 the 2-D contour and 1-D profile of $\cos(2\pi\ \beta f^2 - \theta/2)$ curve, β=0.67 , $\theta = 235^{\circ}$

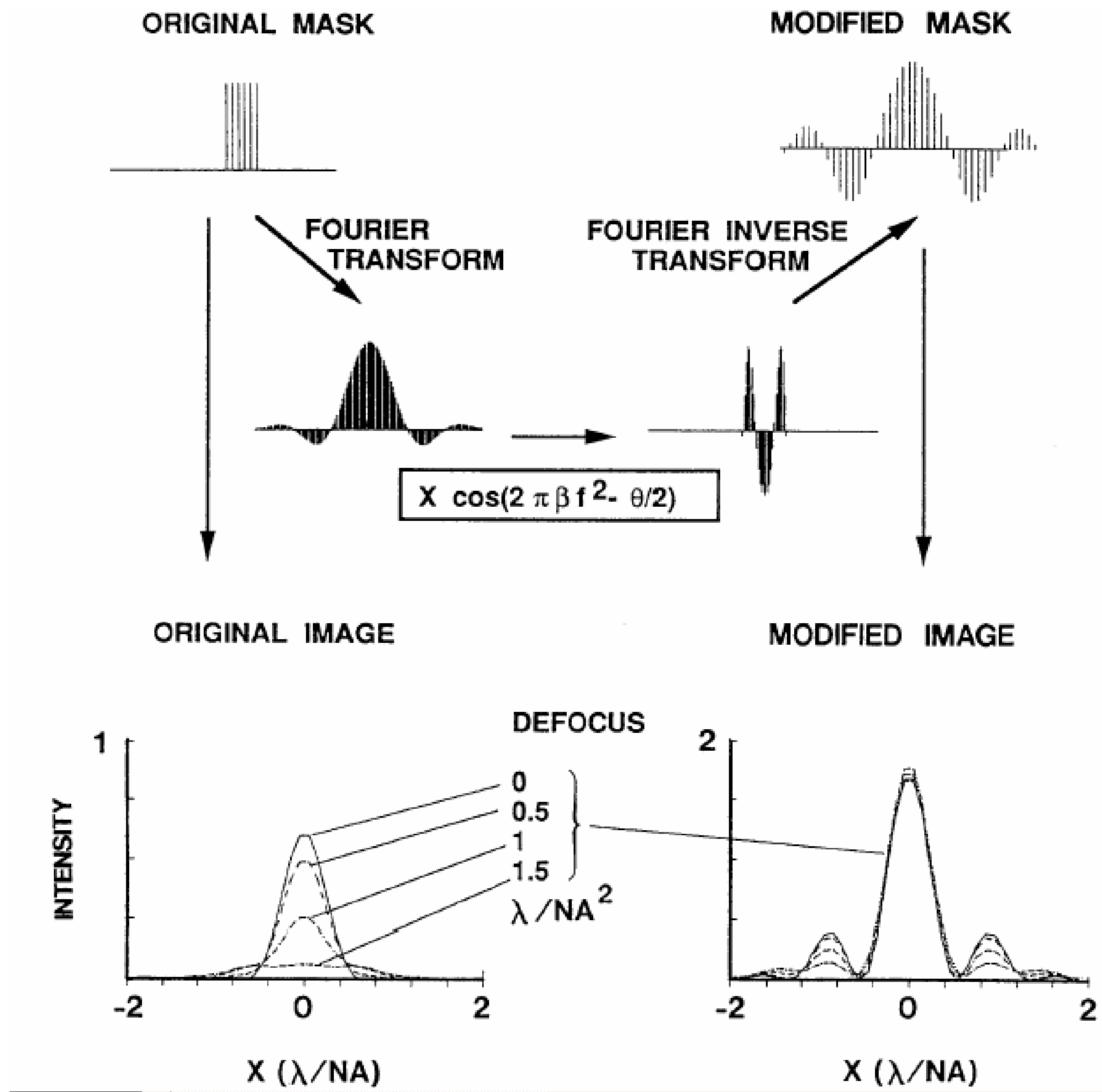

Figure 3-8 Principle of the mask modulation method for the Super-FLEX effect.

Figure 3-9 The result of the modulated pattern contour and profile

calculated by computer program.

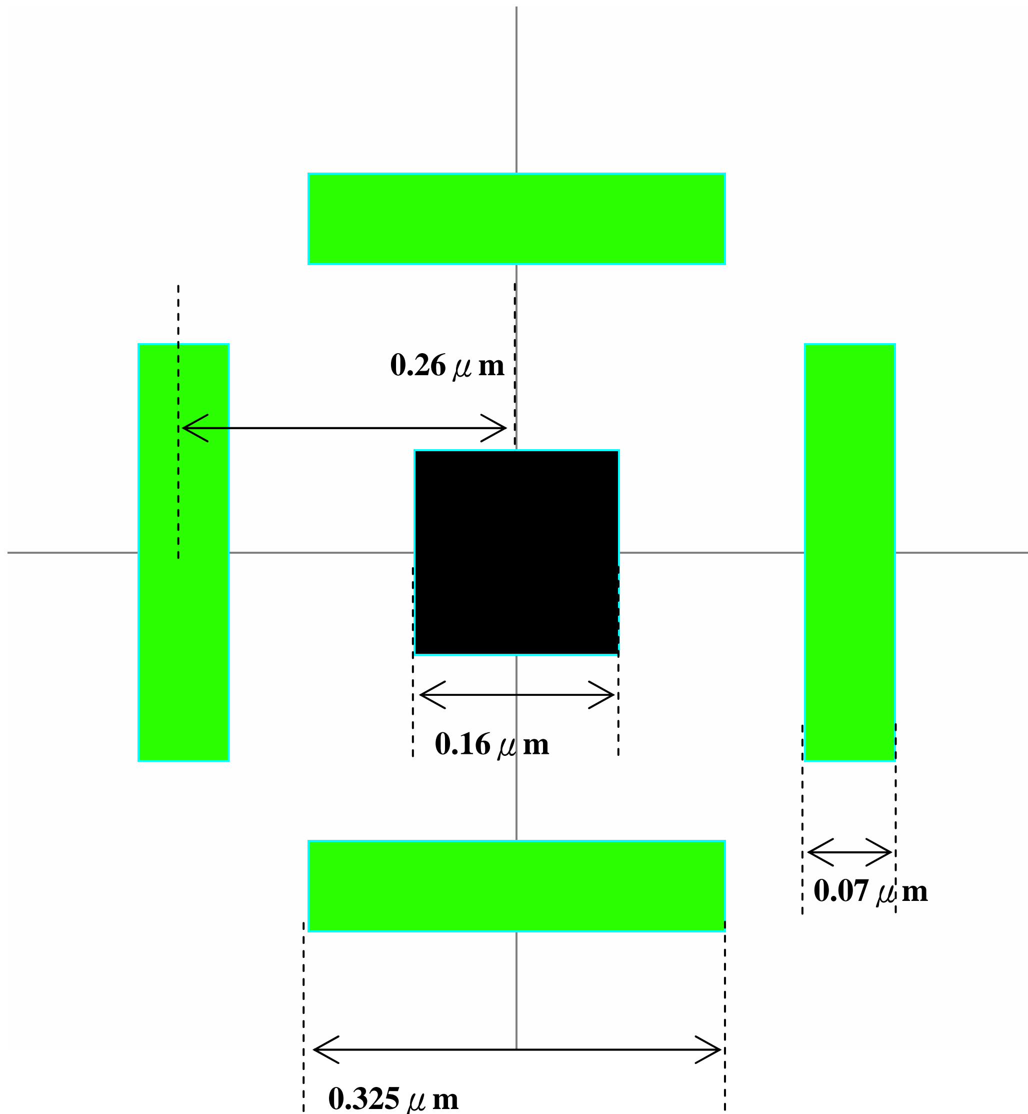

Figure 3-10 The result of the modulated pattern contour and profile calculated by computer program. (the center square are 100% transmissible with 0° phase , and the four out-trigger are 100% transmissible with 180° phase, the else region is opaque.)

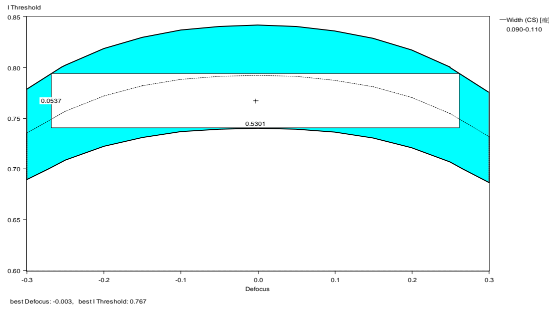

σ=0.1 ,

DOF= 0.5301 μm

best Intensity_threshold = 0.767

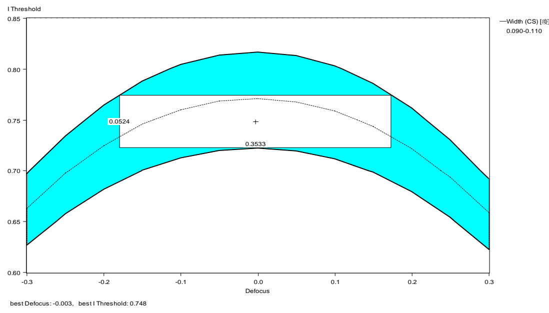

σ=0.2 ,

DOF= 0.3533 μm

best Intensity_threshold = 0.748

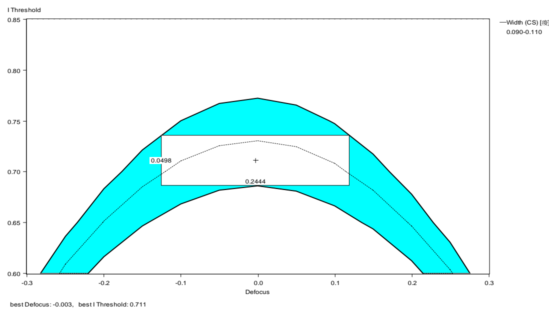

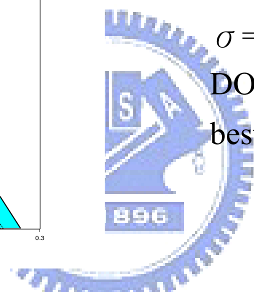

σ=0.3 ,

DOF= 0.2444 μm

best Intensity_threshold = 0.711

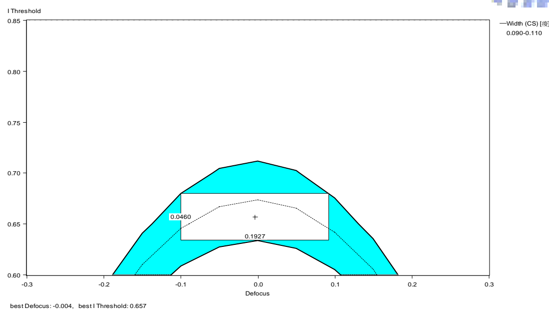

σ=0.4 ,

DOF= 0.1927 μm

best Intensity_threshold = 0.651

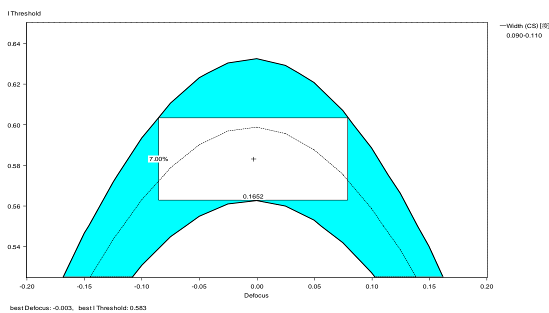

σ=0.5 ,

DOF= 0.1652 μm

best Intensity_threshold = 0.583

Figure 3-11 The E-D curve of the 100nm contact-hole pattern which is modified by the result of the modulated pattern, set EL=7%.

QUASAR (rot. 45 deg.)

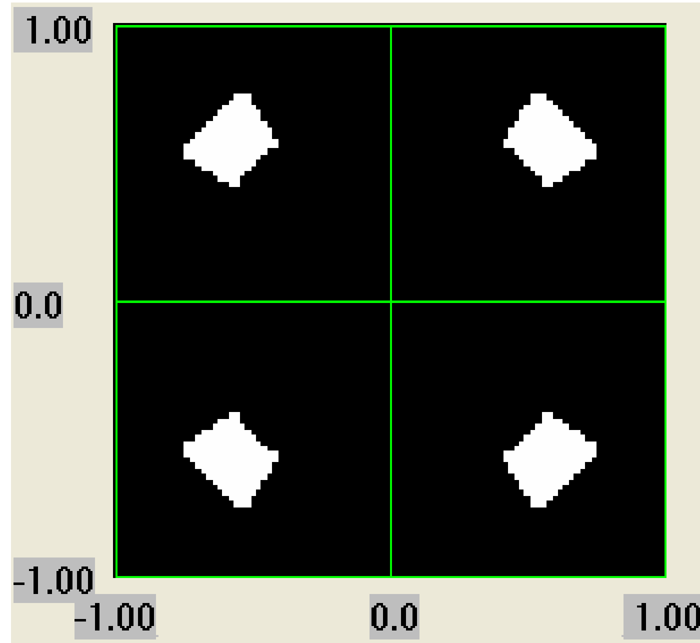

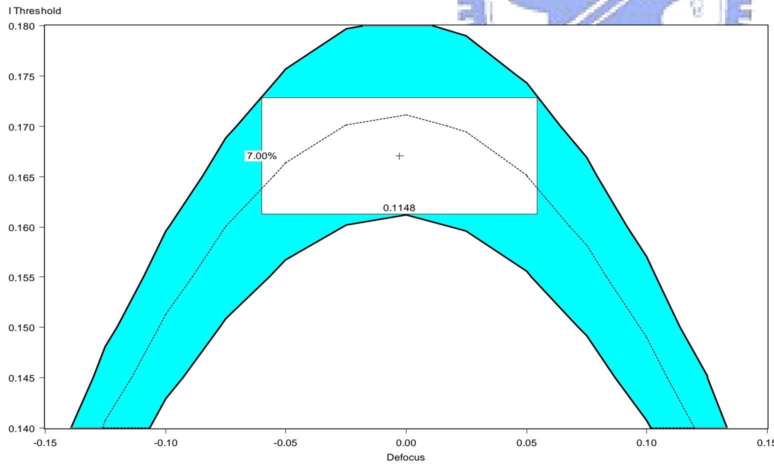

Width (CS)
0.090-0.110

QUASAR rotation 45 deg. ,
spread angle : 20 deg.
Outer radius: 0.93
Inner radius: 0.7

DOF= 0.1148 μm
best Intensity_threshold = 0.167

Figure 3-12 The E-D curve of the 100nm contact-hole pattern using the mask modulation method with OAI, set EL=7%.

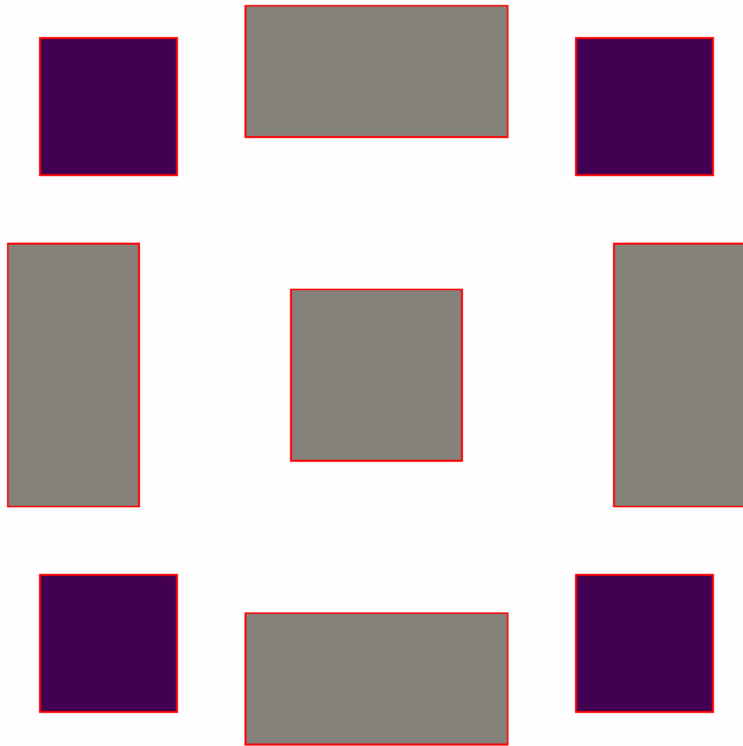

Figure 3-13 Our contact-hole pattern design
(the center square are 100% transmissible with 0° phase , and the four out-trigger are 100% transmissible with 0° phase, the four square phase-shifting AF are 100% transmissible with 180°,else is opaque.)

[university logo watermark]

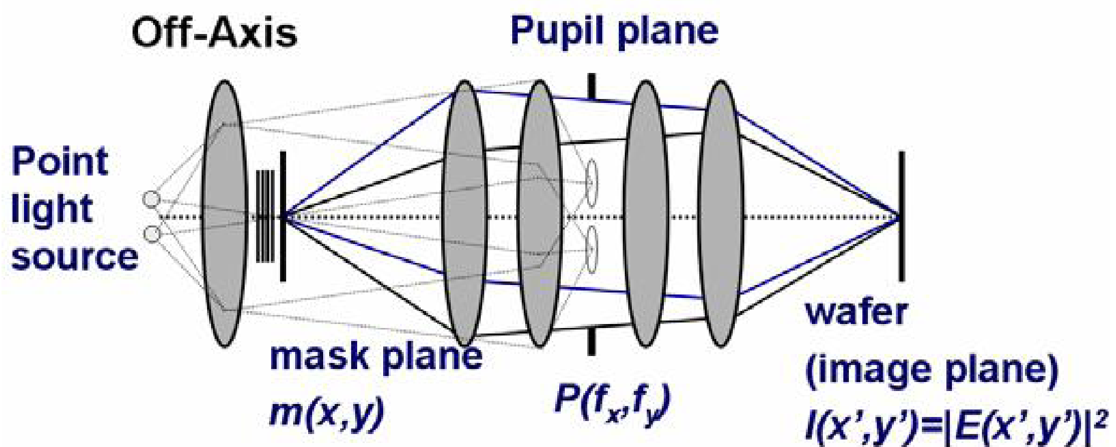

Figure 3-14 Modeling and analysis of OAI projection system.
Mask pattern m(x,y) on the object plane received oblique incidence by partially coherent illumination creating an diffraction distribution

$$a(f_x - f_{sx}, f_y - f_{sy})$$

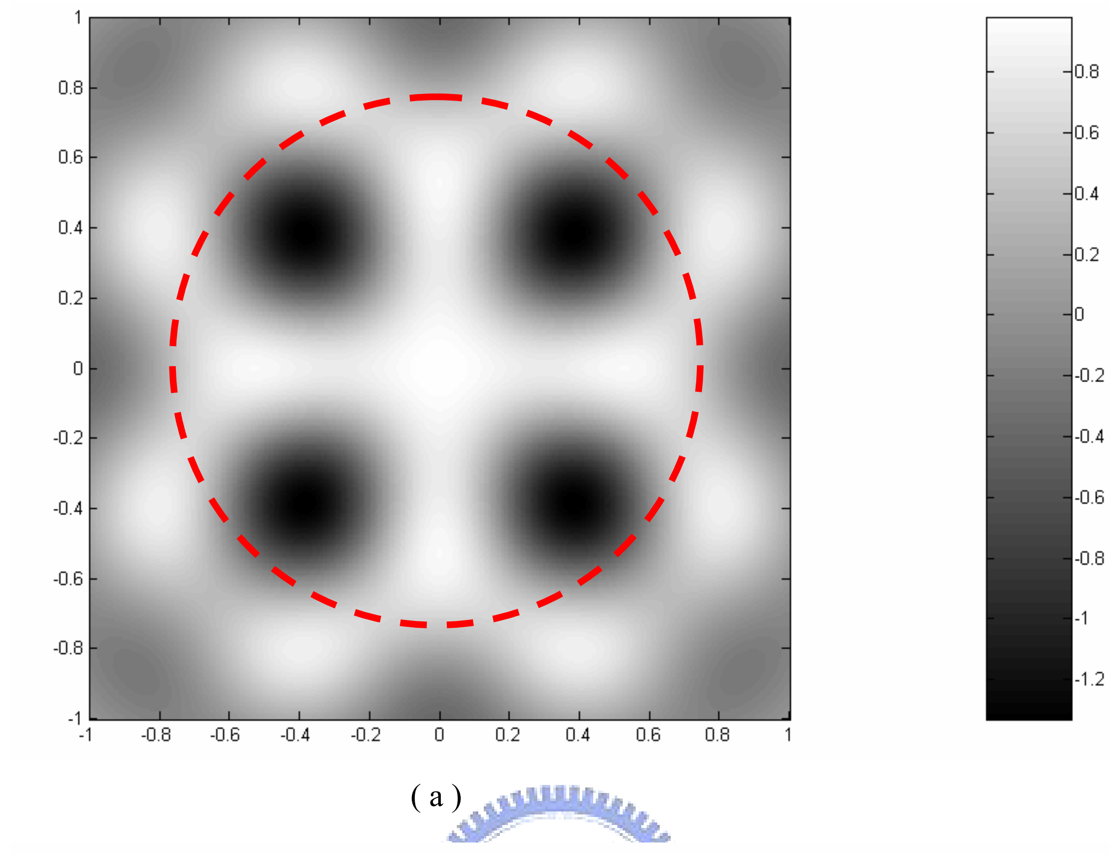

(a)

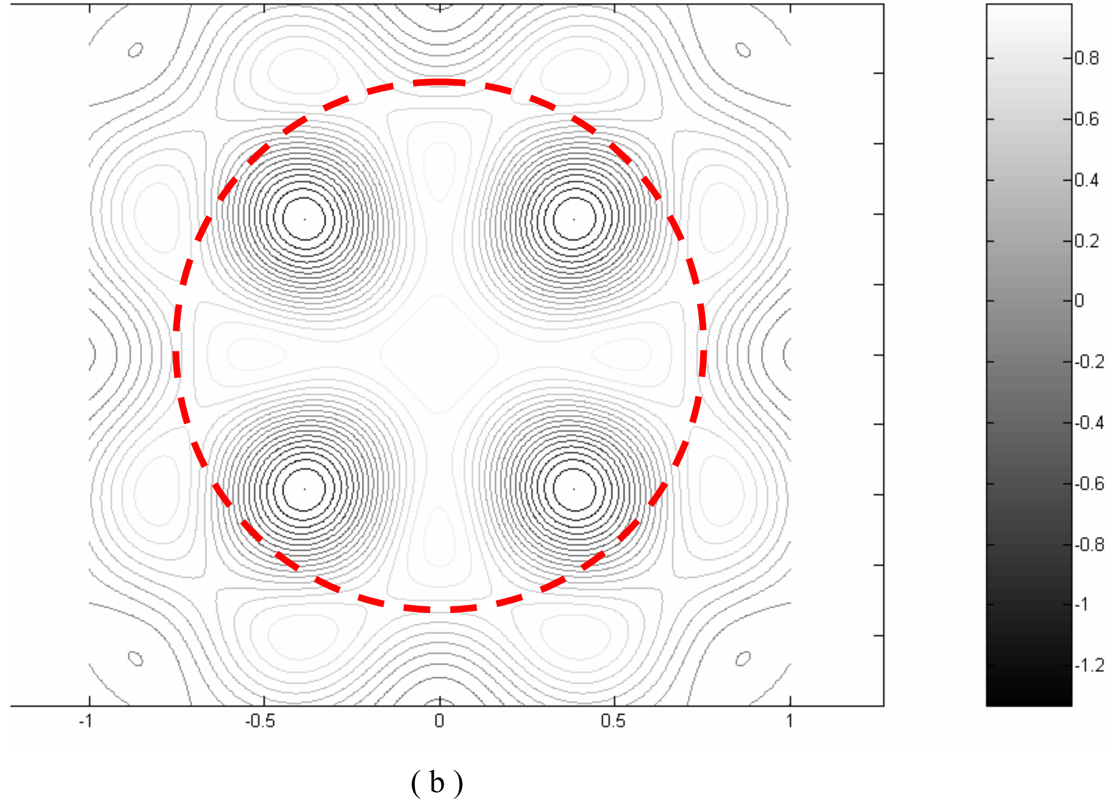

(b)

Figure 3-15 The Fourier transform image of our design on the pupil plane with conventional illumination. (the dash circle represents the pupil.) (a) continuous distribution (b) contour .

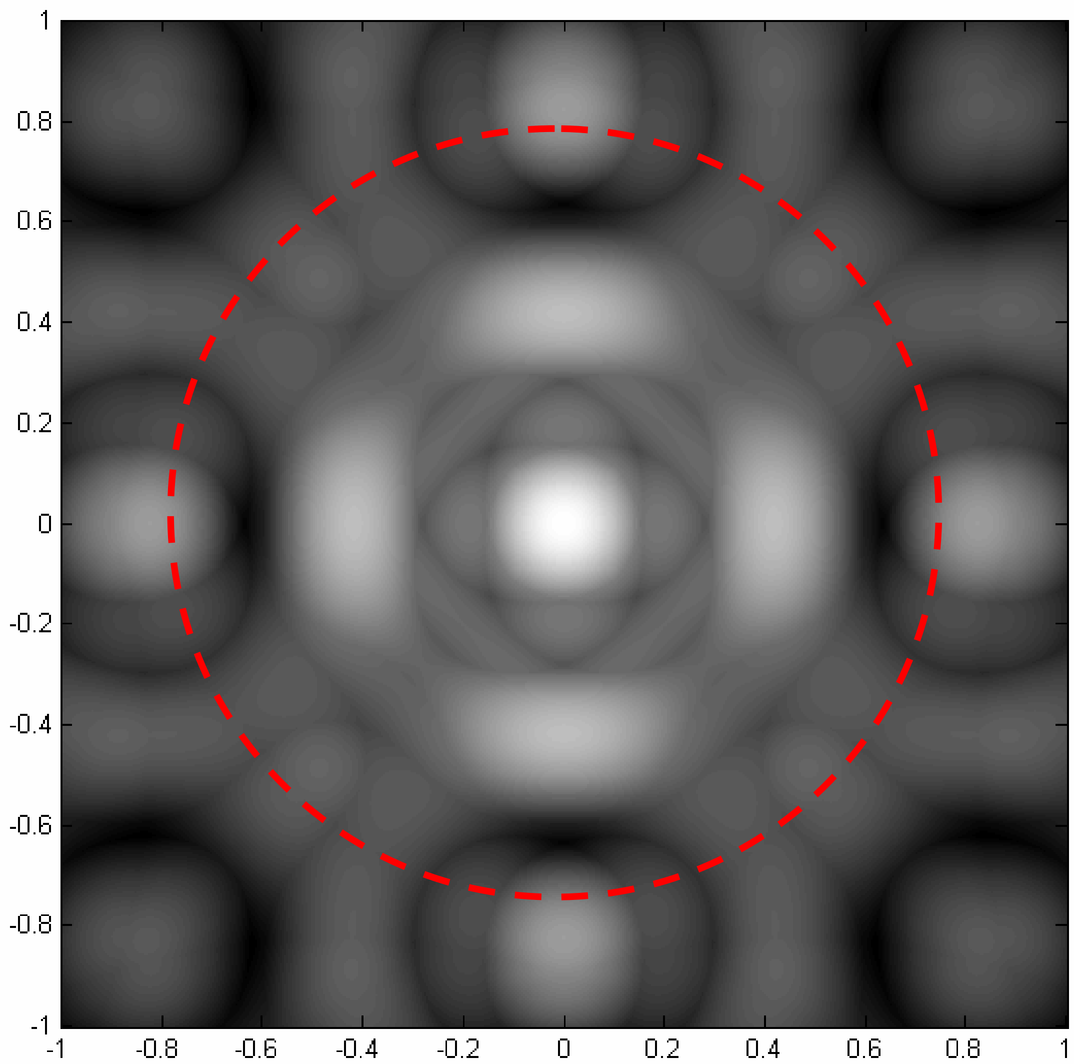

Figure 3-16 The spectrum image, on projection pupil plane, of our pattern design with OAI . (the dash circle represents the pupil.)

Chapter 4

Discussion and Conclusions

4.1 Discussion

When we testing the β parameter, we see the phenomenon like **[Figure 4-1]**.It is seems that the relation of increament of β and increament of DOF is not linear. We find that β have a optimum value to make DOF be maximum but will suffer the EL althought it is always in the acceptable region.

And we find that, the increment of the DOF is seems to be "pulled" outward from the area of the center region, so the center region will be thiner and thiner. Also it is just like two merged process window chart when β is small, and this is match to the original motive of the FLEX method by multi-focal plane exposure.

When we use our design with OAI to improve DOF, there is also the similar phenomenon, but we have not find the exact mechanism , because both the phase-shifting AF and the ASB will affect the DOF and theEL, even the design spec of the main contact-hole will affect,too.

Compare our design with ASB using OAI, our design is indeed better, although the parameters of our design need to optimum is more.

4.2 Conclusions

In this thesis, we present a new contact hole PSM design,which will be compatible with dense contact-hole. When it is applied together with QUASAR OAI, we can enhance the printing resolution to achieve an excellent overall process window for printing contact feature CD below sub-half exposure wavelength. The imaging quality enhancement mechanism for our design is to use it together with QUASAR illumination to form a natural pupil filter that is functionally behaved like the previously presented “Super-FLEX “effect. Using this design with OAI is a much more elegant and flexible approach than to insert an actual pupil filer to the lens to form Super-FLEX.

Although we have demonstrated excellent printing perform for isolated contact hole, we show that this method call for additional illumination optimization in order to achieve optimized results for printing through-pitch, random array of contact hole patterns.

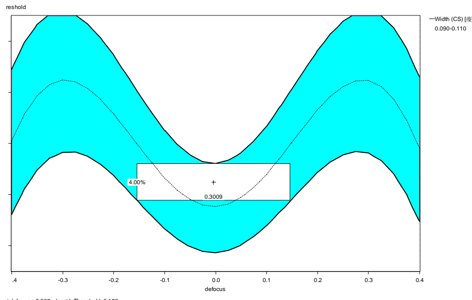

σ =0.1 ,
β = 0.700
DOF= 0.301 μ m
best Intensity_threshold = 0.182

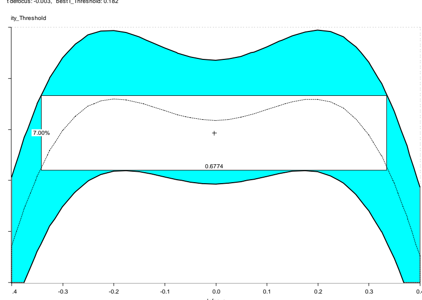

σ =0.1 ,
β = 0.670
DOF= 0.6774 μ m
best Intensity_threshold = 0.209

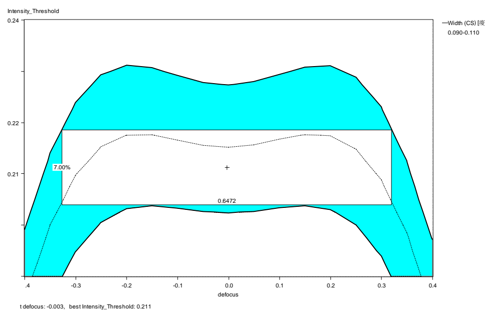

σ =0.1 ,
β = 0.667
DOF= 0.6472 μ m
best Intensity_threshold = 0.211

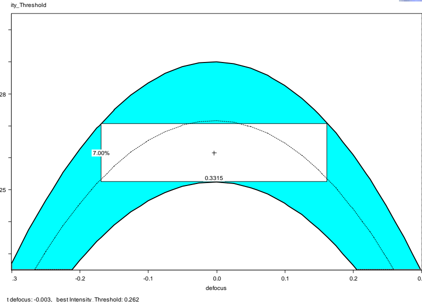

σ =0.1 ,
β = 0.634
DOF= 0.3315 μ m
best Intensity_threshold = 0.262

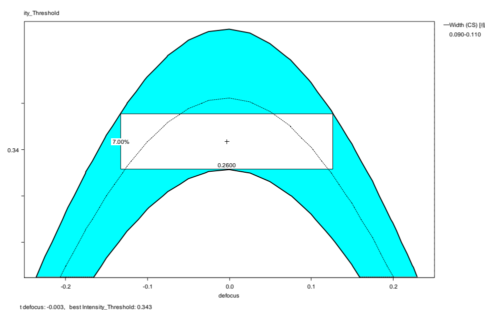

σ =0.5 ,
β = 0.568
DOF= 0.26 μ m
best Intensity_threshold = 0.343

Figure 4-1 E-D curve of 100nm contact-hole using BIM with lens pupil filtering method. .

References

[1] Smith, B.W. and Sheats, J.R., eds., Microlithography: Science and Technology, ch. 3, Marcel Dekker, Inc., 1998

[2]F.M. Schellenberg, "Resolution Enhancement Technology: The Past, the Present, and Extensions for the Future," Proc. SPIE, Vol. 5377, pp. 1-20, 2004.

[3]L.W. Liebmann, "Layout Impact of Resolution Enhancement Techniques: Impediment or Opportunity?" Proc. ISPD'03, April 6-9, Monterey, CA, pp. 110-117, 2003.

[4] P. Jedrasik, "DOF Imporvement by complex pupli filtering for DUV lithography," Proc. of SPIE. vol. 3679, pp. 800- 811, 1999.

[5]Levenson, M. D. *et al*. "Improving resolution in photolithography with a phase-shifting mask." *IEEE Trans. Electron Devices* **29**, pp.1828-1836, 1982.

[6]Terasawa, T. *et al*. "0.3 μm optical lithography using a phase shifting mask." *Proc. SPIE* **1088**, pp.25-33 ,1989.

[7]Matsuo, K. *et al*. "High resolution optical lithography system using oblique incidence illumination." *Technol. Digest IEDM* **91**, pp.70-972 ,1991.

[8] H. Kang, C. Kim, J. Lee, W. Han, and Y. Koh, "High performance lithography with advanced modified illumination," IEICE transactions on Electronics, vol. 77-C,

no.3, pp.432-437, 1994.

[9] M. Levenson, N. Viswanathan, and R. Simpson, “Improving resolution in photolithography with phase shift mask,” IEEE Transactions on Electron Devices, vol.29,no.12, pp. 1812-1846, 1982.

[10] K. Toh, G.Dao, R. Singh, and H.Gaw, “Chromeless Phase shifted mask: A new approach to phase shift masks,” Proc. of SPIE vol.1496, pp.27-53, 1990.

[11] B.J. Lin, “The Attenuated PSM,” Solid State technology 35,pp. 43-47,1992.

[12] T. Terazawa, N. Hasegawa, and H. Fukuda, “Imaging characteristics of multi-phase-shifting and half tone phase shifting masks,” Jpn. J. of Appl. Phys., vol. 30. no. 11B, pp.2991-2997, 1991.

[13] H. Fukuda, A. Imai, and S. Okazaki, “Phase shifting mask and flex method for advanced photolithography,” Proc. of SPIE. vol. 1264, pp. 14- 25, 1990.

[14] H. Fukuda and S. Okazaki, “Spatial filtering for depth of focus and resolution enhancement in optical lithography” ,J. Vac. Sci. Technol. B9 (6), pp. 3113- 3116, Nov/Dec 1991.

[15] J.W.Goodman; "Introduction to Fourier Optics", McGraw-Hill, San Francisco 1968.

[16] H. Fukuda, T. Terasawa, and S. Okazaki, “Spatial filtering for depth of focus and resolution enhancement in optical lithography”, J.Vac. Sci. Technol. B9 (6),1991

[17] Hiroshi Fukuda, Y. Kobayashi, K. Hama, T. Tawa, and S. Okazaki, "Evaluation of Pupil Filtering stepper-lens system", Jpn. J.Appl. Phys. 32, 5845 ,1993.

[18] Hiroshi Fukuda "Axial imaging Superposing (Super-FLEX) Effect Using the Mask Modulation Method for in High-Numerical Aperture I-Line Lens", Jpn. J. Appl. Phys. 30, 3037 ,1991.

[19] Oberhettinger, Fritz;" Tables of Fourier transforms and Fourier transforms of distributions", Berlin/Springer-Verlag, 1990

[20] B. W. Smith, "Forbidden Pitch or Duty-Free: Revealing the Causes of Across-Fitch Imaging Differences", Proc. of SPIE vol. 5040, pp399-407, 2003.

[21] Chang, Chung-Hsing "Novel contact hole reticle design for enhanced lithography process window in IC manufacturing" ,Proc. of SPIE. vol. SPIE-5645, pp.32-43. 2005